CHAPTER 4

STANDARD ENGINEERING PROPERTIES OF BRINGELLY SHALE

§4.1 INTRODUCTION

In this chapter some of the basic physical properties such as porosity and dry density, natural water content, specific gravity of particles, and bulk density are reported.

Liquid limit and plastic limit tests have been performed on pulverized samples of Bringelly shale from the four sites under study. The study has covered material ranging from fresh to extremely weathered. The clay size fraction was determined from sedimentation analysis and limit test results have been related to the clay mineralogy of the material.

To investigate the mechanical properties of Bringelly shale, simple index tests on intact shale specimens were performed. These have included unconfined compression strength tests, point load index tests, and slake durability tests. This chapter summarises the findings of these strength tests and examines the degree of breakdown of the shale upon drying and wetting. A correlation between the results of uniaxial compression tests and point load test is established, and the effects of mineralogy and cementation on the strength of the rock have also been investigated.

In this chapter, a description of the laboratory tests including the test results of different properties for Bringelly shale are individually presented in the following sections. All test data are used in analysis and interpretation of the results however, only representative test results are shown in figures and tables.

§4.2 TESTING OF PHYSICAL PROPERTIES

This chapter gives details of the testing on intact specimens of Bringelly shale at various degrees of weathering. Tests to investigate the fundamental properties; water content, density, porosity, material consistency, and clay content have been performed. These properties are closely interrelated and are essential to understanding the relationships between the different standard properties of Bringelly shale. The ISRM (1979b) suggested methods for measuring these properties have been followed in this study.

§4.2.1 Water content

The water content (w_c) of a rock can significantly influence its mechanical behaviour. In shale rocks, it has been well established that the water content can have a significant effect on their strength and stiffness (e.g. Hsu & Nelson, 1993; Ghafoori, 1995; Lashkaripour & Ghafoori, 1999).

To compare Bringelly shale from the four sites considered in this work, samples with different degrees of weathering i.e. fresh, moderately, and extremely weathered shale were selected. Sampling was carried out in accordance with the field guide on engineering classification scheme (Underwood, 1967). The natural water contents of sixty samples were determined (ISRM, 1979a). Values of water mass contained in each rock specimen were determined as a percentage of the oven-dry sample mass. The natural water contents of sixty samples were determined and representative values are presented in Table 4.1. They indicate that the water content of fresh Bringelly shale ranges between

Table 4.1 Water content at different degree of weathering for the Bringelly shale (*KC*: Kemps creek, *BC*: Badgreys creek, *HP*: Horsley, Park, *ML*: Mulgoa)

Sample Number	Water content (%)							
	Fresh samples				extremely weathered samples			
	KC	BC	HP	ML	KC	BC	HP	ML
1	1.78	1.92	2.7	2.2	6.13	6.01	5.04	5.12
2	2.1	2.17	2.57	2.17	5.98	5.93	5.11	4.77
3	2.47	2.71	2.09	2.51	5.03	5.76	4.96	4.66
4	2.69	2.05	2.87	2.65	6.32	4.89	4.36	5.09
5	2.34	2.22	2.3	2.03	6.04	5.01	5.28	5.16

1.78% and 2.87% with a mean value of 2.3% and a standard deviation of 0.28%. The water content of the shale increases as the material weathers. This was indicated by the higher water contents of the extremely weathered shale, which had a mean value of 5.2%. No significant difference in water contents between the different sites was detected.

In order to display the effect of weathering on the natural water contents, the water contents of samples from the four sites at different degrees of weathering were plotted against the corresponding water contents (Figure 4.1). The graph shows the range of natural water contents at each degree of weathering. The different mean value at each state of weathering clearly demonstrates the influence of weathering on the water content of Bringelly shale. The weathering seemed to be decreasing with increasing depth below the surface.

It is worth mentioning that the depth to the ground water is around 35 *m* at all four sampling locations and the shale is only partly saturated (further discussion below) . This may in part reflect the influence of the surface clay that is the end product of completely weathered Bringelly shale. This surface forms a capping layer that minimizes infiltration

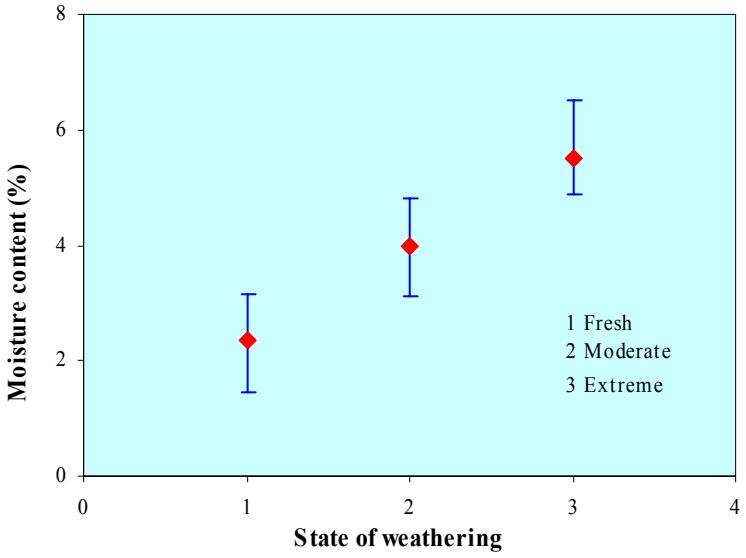

Figure 4.1 Influence of weathering on water content of Bringelly shale

and acts as a confining unit to the groundwater in many parts of Bringelly shale. This creates local environmental conditions near the surface that could influence the potential evapotranspiration of this layer and lead to variations in the degree of salinity and saturation of the specimens (MacNally, 2004). One of the consequences of the partial saturation is that correlation with other properties and water content will be difficult to establish.

§4.2.2 **Porosity and dry density**

The porosity (n) is the volume of the pore space expressed as a percentage of the total volume of the sample. A closely related property is the void ratio e, that is the ratio of the volume of the voids to the volume of the solids. Porosity is an important property of soils and rocks particularly in the fields of geophysics, rock mechanics, soil mechanics, and petroleum engineering.

There are several different methods that can be used for the direct determination of porosity. However, because of concerns that the samples would disintegrate during sample preparation, and during immersion in water, these were not pursued. In this study, porosity has been determined from the mass and volume knowing the specific gravity of the soil grains.

In order to achieve a realistic porosity value, specific gravity (G_s) was determined in the laboratory. Sub-samples from the dry density test were used in testing for the specific gravity in accordance with the British standard BS 1377: 1977. A calculated mean value of 2.65 was obtained for G_s.

The dry density of Bringelly shale was determined using the water displacement method (BS 1377:1975, Test 15F) as the specimens can be protected by paraffin wax prior to immersing in water. The test method was also used to determine the degree of saturation in Bringelly shale. All samples prepared for the dry density test had irregular geometries. In order to minimize the influence of experimental error, all samples were prepared at a convenient size and shape. The paraffin wax coating allowed the bulk volume of the samples to be determined and avoided the swelling and disintegration of the samples that occurs when placed in water.

Based on the experimental results of specific gravity and dry density, void ratios, porosity, and degree of saturation for Bringelly shale were calculated from the following equations**,**

$$e = \frac{G_s \rho_w}{\rho_d} - 1 \qquad (4.1)$$

$$n = \left(\frac{e}{1+e} \times 100 \right)\% \qquad (4.2)$$

$$S = \frac{w_c G_s}{e} \qquad (4.3)$$

Based on the assumption that the density of water ρ_w is $1\,t/m^3$, the void ratio (e) was found to be in the range of 0.06 to 0.16, while the degree of saturation (S) of Bringelly shale was found to be in the range of 21% to 90% with a mean value of 66%.

The pore volume was calculated from the difference in bulk and grain volumes. The porosities of twenty four samples of fresh Bringelly shale from the four sites were determined. The dry densities (ρ_d) of fresh shale samples considered in this study range from 2.29 to 2.47 t/m^3, and the mean dry density was calculated to be 2.4 t/m^3, with a standard deviation of 0.07 t/m^3. Porosity of fresh Bringelly shale ranges between 5.25% to 13.74% with the Mulgoa site having the lowest values and the Horsley Park site, the highest values. Representative results from the laboratory tests and calculated parameters are illustrated in Table 4.2

The empirical measurements indicate that all samples of the Bringelly shale were only partially saturated in situ. Given the difference in the mean values of saturation of Bringelly shale at different sites, it is believed that fluctuations of water table and varying ground water conditions across the different sites are the main contributors for such a variation. The difference in saturation of samples from the four sites also suggests that the block samples, which were obtained from the floor of active quarries may have been exposed for different times. The core samples from Kemps Creek showed higher degree of saturation compared to those measured from the block samples obtained from the same site supporting the suggestion that the water flushing used during coring may influenced the specimens saturation, or the block samples had dried out to some extent.

Similar tests on Ashfield shale indicated that fresh samples were essentially fully saturated (Ghafoori, 1995). Because of the similarity of porosity and environmental conditions it is believed that the lower saturation of the Bringelly shale is related to microcracking in Bringelly shale which is absent in Ashfield shale. As these microcracks would be expected to open during coring and sample preparation it is reasonable to

Table 4.2 Representative porosity and dry density of Bringelly shale from all sites

Sample Name	Bulk density (t/m^3)	Specific gravity	Dry density (t/m^3)	Porosity %	Moisture content %	Saturatiom (S%)	Mean (S%)
K1	2.52	2.65	2.46	7.31	2.59	87	
K2	2.48	2.65	2.40	9.49	3.55	90	
K3	2.45	2.66	2.37	10.45	3.42	78	
K4	2.40	2.64	2.33	12.12	2.77	54	73
K5	2.42	2.65	2.36	11.09	2.91	62	
K6	2.45	2.64	2.37	10.33	3.11	71	
B1	2.41	2.64	2.37	10.64	1.89	42	
B2	2.33	2.66	2.30	13.18	1.22	21	
B3	2.47	2.67	2.44	7.92	1.09	34	
B4	2.42	2.65	2.38	10.27	1.63	38	
B5	2.43	2.66	2.39	9.78	1.61	40	40
B6	2.51	2.67	2.47	6.78	1.58	56	
B7	2.52	2.65	2.49	5.97	1.27	53	
M1	2.50	2.66	2.45	7.53	1.95	64	
M2	2.45	2.64	2.41	8.93	1.67	45	
M3	2.54	2.65	2.49	5.85	1.80	76	
M4	2.55	2.65	2.51	5.41	1.90	88	70
M5	2.55	2.66	2.51	5.25	1.77	84	
H1	2.44	2.64	2.38	10.22	2.56	60	
H2	2.41	2.67	2.35	11.39	2.65	55	
H3	2.42	2.65	2.35	11.44	3.28	67	
H4	2.42	2.64	2.35	11.25	2.88	60	58
H5	2.40	2.66	2.34	11.75	2.76	55	
H6	2.35	2.65	2.29	13.74	2.95	49	

K :Kemps Creek B:Budgreys Creek M: Mulgoa H: Horsley Park

expect higher degree of saturation in-situ. The test results have shown that the water content of Bringelly shale should not be used as a direct measure of its porosity. It may also be noted that the lowest porosity value of Bringelly shale is among the minimum values reported for shales from around the world (cf. Bell, 1981).

A plot of dry density versus water content is illustrated in Figure 4.2. It shows that dry density decreases with an increase in water content. The plot also indicates that there is wide scatter in the data due to the incomplete degree of saturation, this was evident from the result of regression analysis that shows a significant low value of the correlation coefficient with $r^2 = 0.17$.

The bulk density of Bringelly shale was also determined. Forty samples were tested in the laboratory for this purpose. The test results indicated that bulk densities range from 2.35 t/m^3 to 2.55 t/m^3 with a calculated mean value of 2.48 t/m^3.

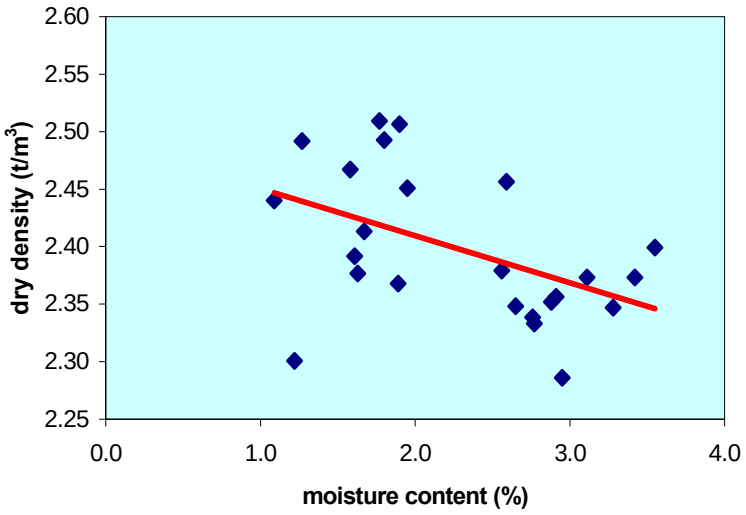

Figure 4.2 Dry density versus water content for Bringelly shale

§4.2.3 **Particle size analysis**

A standard hydrometer test was employed in this study to analyse the particle size distribution of the Bringelly shale. The analysis involved crushing of intact material in a ball mill. The shale was crushed until it all passed a 75 μm mesh sieve. Samples of four different degrees of weathering were tested to determine their clay size fractions. Hexametaphosphate solution at a concentration of 4% was used to disperse the samples. All tests were performed at a temperature of 20 °*C*.

Sedimentation analysis, using *Stokes's law* was adopted to determine the clay content of Bringelly shale. Samples ranging from fresh to extremely weathered shale from Kemps Creek were used in this study. The Australian standard procedure (AS 1289.3.6.3, 1994) was adopted to determine the clay fraction less than 2 μ. The procedure utilizes the relationship among the velocity of fall of spheres in a fluid, the diameter of the sphere, the unit weight of the sphere and of the fluid, and the viscosity of that fluid. Calculation of clay fraction is based on Stokes expression:

$$\nu = \frac{2}{9}\frac{\gamma_s - \gamma_w}{\eta}\left(\frac{D}{2}\right)^2 \qquad (4.4)$$

where:

ν = velocity of fall of the spheres, cm/sec

γ_s = unit weight of the sphere, g/cu cm

γ_w = unit weight of the fluid, g/cu cm, usually water

η = absolute viscosity of the fluid, dyne-sec/sq cm

D = diameter of the sphere, cm

The grain size distribution is shown in Figure 4.3, from which it can be seen that the contents of clay, fine to medium silt, and coarse silt are 55%, 30% and 15%, respectively.

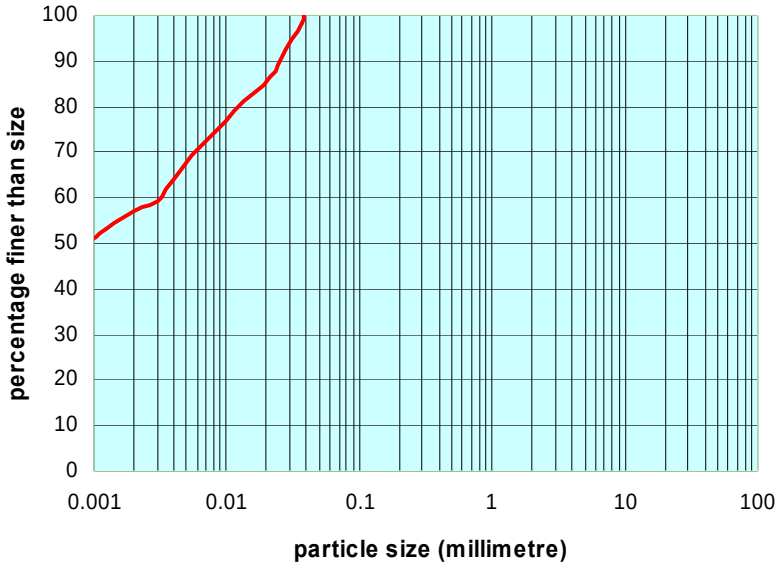

Figure 4.3 Grain size distribution analysis of fresh Bringelly shale (<75 μ m fraction)

In this test, only particles with sizes finer than 75 μ were involved in the analysis. The results from the sedimentation analyses indicated an increase of 6% in the clay fraction as the shale becomes more weathered. Sedimentation showed that fresh shale has a clay content of about 52% which agrees with the 51% clay fraction determined from the mineralogical studies. The increase in clay fraction to 58% upon changing the weathering state from fresh to extremely weathered could be attributed to 2 mechanisms:

(i) the break down of larger kaolinite (0.5-5 μ) particles.

(ii) the breakdown of illite/mica aggregates that have been cemented together by recrystallisation, as shown by the microscopic analyses. Under the influence of extreme weathering, these particles can be broken down into finer grains (<2 μ) and hence increase the clay fraction as detected by the sedimentation test.

These mechanisms are based on the assumption that the breaking down of the clay is a physical process, and not apparently associated with a change in clay mineral content. It has been shown in Chapter 3 that the clay mineral content remains approximately constant. However, there is little unweathered material such as feldspars that could be transformed into clay by weathering..

The results obtained from the quantitative analysis of the clay minerals, based on interpretation of x-ray diffraction analysis have shown that percentage of kaolinite in the clay minerals has increased from 30% for the intact rock to 33% in the extremely weathered shale (Chapter 3). Despite the insignificant increase in kaolinite however, it may substantiate the fact that the fusion of clay particles particularly the mixed-layer clays (*K*+*Ch*) may form clumps of particles or grains of silt size. As the rock is progressively subjected to a substantial degree of weathering from fresh to extremely weathered state, these clumps of silt size grains may be broken down to finer clay size grains and clay particles.

This process is believed to be the main cause for the apparent increase of the clay fraction in the extremely weathered material. This increase in fines may also contribute to the increase in liquid limit and plasticity index of the weathered Bringelly shale. The influence of degree of weathering on clay fraction is plotted and presented in Figure 4.4.

Representative samples from the four sites at four different grades of weathering were tested for determining the clay content of less than 2 micron. Each plotted point is an average of four test results from one of the four sites. The figure shows the average increase of clay fraction (less than 2μ) as the rock progresses to a more advanced weathering state.

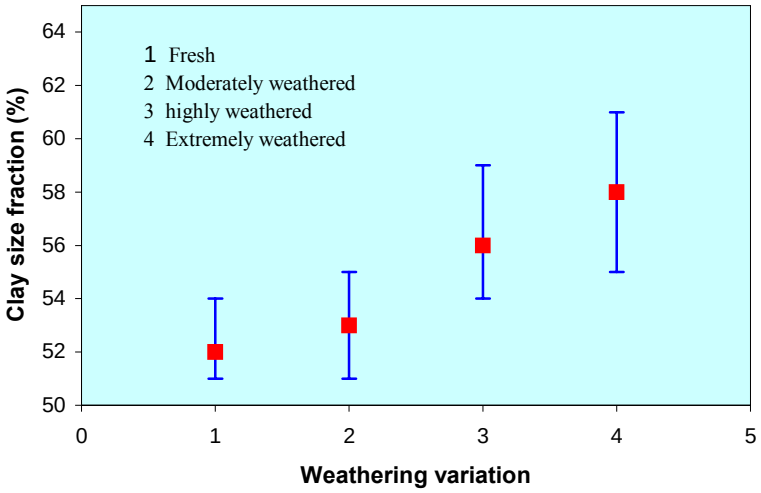

Figure 4.4 Influence of weathering variation on the clay fraction less than 2 μ

§4.2.4 **Atterberg limits**

Atterberg limits tests have been performed on samples from Bringelly shale. These tests are often performed to provide data on mineralogy and clay content and to study the influence of weathering.

In order to determine the liquid and plastic limits of Bringelly shale, all samples were ground in a ball mill for two minutes. The Australian standard procedures (AS 1289.3.1.1&3.1.2, 1995) for the determination of the liquid and plastic limits were adopted. A total of 32 liquid and plastic limits tests were carried out on specimens with different degrees of weathering from the four sites. For every test after determining the plastic limit (w_p) and liquid limit (w_l), the plasticity index (I_p) was calculated using the following formula:

$$I_P = w_L - w_P \qquad (4.5)$$

The results of these tests indicated that crushed remoulded fresh Bringelly shale has low plasticity, ranging from a plasticity index of 7.1 to 12.3. However, points with higher plasticity indices were obtained from material subjected to weathering. A summary of Atterberg limits for Bringelly shale is given in Table 4.3.

Based on the Atterberg limits, the remoulded Bringelly shale at all states of weathering has the physical characteristics of inorganic clays of low to medium plasticity (*CL*). The relationship between plastic limit and liquid limit of all samples with fresh and extremely weathered states of weathering shown in Figure 4.5, exhibits a clear trend. This trend shows that increasing liquid limit is associated with an increase in the plastic limit and subsequent increase in the plasticity index (Fig. 4.6). The Figure shows that the extremely weathered samples from Bringelly shale are increasingly above the *A*-line of the plasticity chart, as the plasticity increase with the increase of the degree of weathering**.**

It has been shown that increasing degree of weathering is associated with increasing water content and increasing liquid limit and also subsequent increase in the clay fraction. The results also showed that there is a clear trend of increasing plasticity index with increasing clay fraction (Fig. 4.7). As noted the increase in plasticity index is associated with an increase in liquid limit and hence the water content. In the mean time, considering the influence of clay mineralogy on the Atterberg limits, the pattern in figures 4.4 and 4.7 may indicate changes in the clay mineralogy, but not the clay mineral fraction, that are regardless of the degree of weathering of the material encountered. However, it has not been possible to establish a significant correlation between water content and liquid limit. This is believed to be a result of the variable saturation of the specimens considering the fact that in situ water content may not represent an intrinsic soil property if compared to Atterberg limits parameters.

This follows the general trend of many shales e.g. Ashfield shale (Ghafoori, 1995) in that weathering increases the clay size fraction. Furthermore, the influence of weathering was

investigated in an effort to establish a link between the property of plasticity and the clay sized fraction of Bringelly shale.

Table 4.3 Atterberg limit test results of fresh and weathered Bringelly shale

Sample Name	Fresh shale			Extremely weathered shale		
	Liquid limit (%)	Plastic limit (%)	Plasticity index (%)	Liquid limit (%)	Plastic limit (%)	Plasticity index (%)
BC1	30	18.5	11.5	46	12.2	33.8
BC2	30	21.1	8.9	38	14.9	23.1
BC3	32	21.2	10.8	42	11.0	31.0
BC4	33	24.6	8.4	43	16.8	26.2
HP1	29	19.7	9.3	33	14.0	19.0
HP2	29	20.0	9.0	46	15.7	30.3
HP3	30	21.1	8.9	45	12.1	32.9
HP4	35	26.3	8.7	48	15.0	33.0
ML1	32	24.5	7.5	42	17.4	24.6
ML2	30	22.8	7.2	33	11.6	21.4
ML3	28	19.1	8.9	43	17.2	25.8
ML4	31	23.9	7.1	43	13.0	30.0
ML5	28	20.1	7.9	35	17.7	17.3
KC1	30	20.2	9.8	48	15.9	32.1
KC2	27	15.4	11.6	52	15.2	36.8
KC3	37	25.0	12.0	38	15.7	22.3
KC4	32	21.0	11.0	39	18.3	20.7
KC5	35	24.0	11.0	40	14.9	25.1

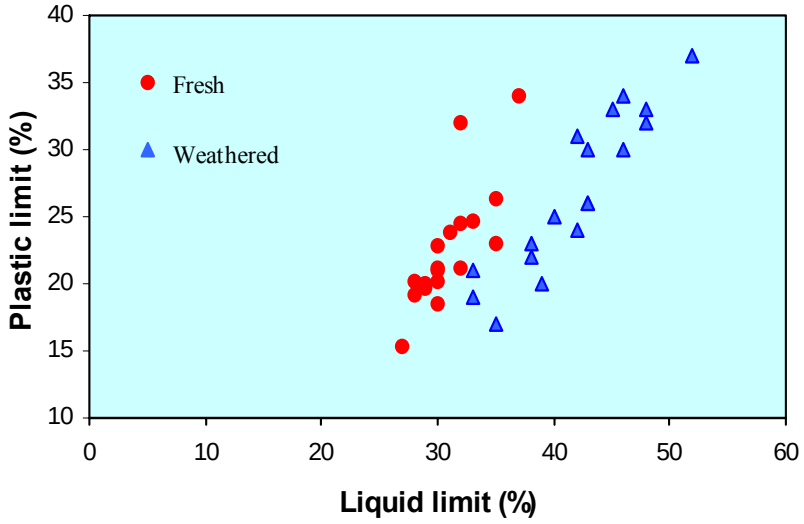

Figure 4.5 General trend of liquid limit and plastic limit of Bringelly shale

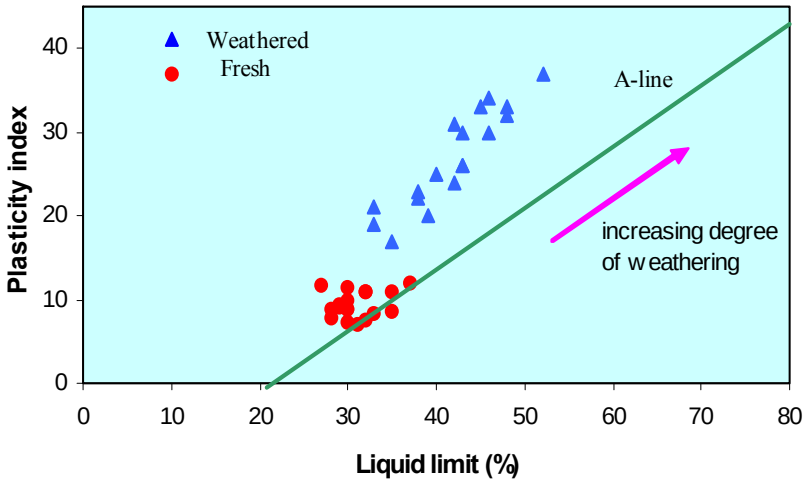

Figure 4.6 Atterberg limits of fresh and weathered Bringelly shale

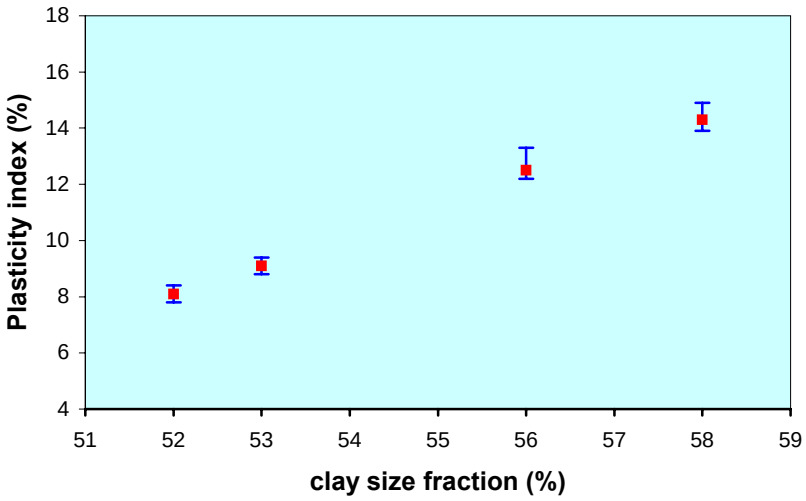

Figure 4.7 Relationship between clay content versus plasticity index under the influence of weathering

This in turn shows that increase in liquid limit is an indication of an increase in the clay fraction due to breakdown of cementation and / or bonding throughout different stages of weathering. The activity of Bringelly shale was determined using the results of plasticity index and clay size fraction (< 2 micron). It is the ratio of the plasticity index to the percentage of soil less than 2 microns. The activity of the clay from the four samples tested at different degrees of weathering varies from 0.15 for fresh material to 0.60 for extremely weathered material. Based on Skempton's classification, the clay in Bringelly shale is described as inactive. This classification seems to ignore the sensitivity property of this material when it is subjected to water or high moisture.

§4.3 TESTING FOR STRENGTH AND DURABILITY

The effects of sample geometry, loading configuration, and degree of weathering on the intact shale rock were studied by performing simple index tests. Uniaxial compression

and deformability, point load index, and slake durability tests were used to investigate the strength and durability of Bringelly shale.

§4.3.1 **Uniaxial compressive strength**

The uniaxial compressive test (*UCS*) is possibly the most broadly used property in rock engineering. The main objective of these tests has been to characterize the uniaxial compressive strength of Bringelly shale, and to assess the relationship between uniaxial compressive strength and various other properties. The tests were performed on cylindrical core specimens using a $250\,kN$ capacity servo controlled testing machine with a cross-head that applies the load required during the test at a rate that can be controlled manually. This machine can be adjusted to apply a constant rate of stress or a constant rate of strain. In the tests reported here the axial load was applied with a constant rate of axial deformation of 0.2 *mm* / minute i.e. a constant cross-head movement rate. The rate was selected on the basis of a nominal time to failure of 10 to 15 minutes from the beginning of loading as recommended by ISRM (1981). In order to reduce the specimen end effect, each specimen was placed between two platens with a steel ball seat in the upper platen. The load and displacement were recorded on a chart recorder. Core samples of 51 *mm* diameter were obtained from the borehole at Kemps Creek site. Selected samples were cut to length with a small diamond saw and their ends were ground by sandpaper to make them smooth and perpendicular to the longitudinal axis as recommended by the standard ISRM procedures.

All specimens tested for uniaxial compression were right circular cylinders with a height to diameter ratio of 2 with an allowed error of ±3mm. Each specimen was carefully placed concentrically between the bottom and top platens.

Measured *UCS* values ranged from 2.4 to $49\,MPa$. These data were obtained from the current study (CS) and also from data obtained by the *Road and Traffic Authority* (*RTA*), *NSW*, and *Coffey Geosciences International Pty Ltd* (*CG*) during works for the construction of the M4 between May Hill and Prospect. The mean strength for a total of 40 samples involved was $22.5\,MPa$, with a standard deviation of 9.3 *MPa*. Although all

specimens were reported to be fresh "unweathered" shale, the water contents of some specimens fell in the range of extremely weathered as indicated in Figure 4.1. The mean *UCS* value of the fresh Bringelly shale samples is close to that previously published by Won (1985) who reported a maximum UCS of 80 MPa and a mean strength of 31 MPa. Based on the strength classification group suggested by the *International Society of Rock Mechanics* (1972), the fresh Bringelly shale samples would be described as strong rock.

To further investigate the effect of water content on the mechanical behaviour of Bringelly shale, a correlation between the UCS results and the water contents of the preserved fresh samples from the current study and from other companies was established. Typical data is shown in Table 4.4. Data points of 20 samples with pre-determined water content and UCS including test results from Ashfield shale (Ghafoori, 1995) were also plotted on the same graph (Fig. 4.8) to enable comparison between the two different shales. Both shales show the general trend of decreasing strength with increasing water content as observed for most argillaceous rocks (Van Eeckout, 1976).

The water contents of the samples were in the range from 1.8% to 6.1% with a mean value of 3.6% and a standard deviation of 2.1%. The figure also shows a weak correlation between uniaxial compressive strength and water content. This graph indicates that the UCS decreases with an increase in the water content. This relationship of the two variables is described by the following equation:

$$UCS = 570\, p_a e^{-0.287 w_c} \qquad (4.6)$$

in which w_c is the water content and p_a is the atmospheric pressure (0.1 MPa). Regression analysis shows that the equation (4.6) fits the data with a correlation coefficient of $r^2 = 0.48$. The apparent similarity of these results may reflect a similarity in the strength of both shales, but in the mean time obscures some important differences in the mechanisms leading to their strength. One of the difficulties with obtaining *UCS*

data for Bringelly shale is that core recovery is low, and thus the number of specimens suitable for *UCS* testing is

Table 4.4 Typical data used in plotting Figure 4.8

Sample No.	Source	Location	*UCS*	M_c %
1	CS	KC	31.59	3.11
2	CS	KC	19.82	2.91
3	CS	KC	8.15	3.91
4	CS	KC	43.34	2.94
5	CS	KC	49.12	2.45
6	CS	KC	37.76	2.61
7	CS	KC	26.85	2.46
8	CG	M4	22.63	3.3
9	CG	M4	32.29	2.2
10	CG	M4	10.98	3.7
11	CG	M4	10.97	3.4
12	CG	M4	12.66	5.6
13	CG	M4	9.97	6.1
14	RTA	M4	14.58	5.8
15	RTA	M4	14.69	5.0
16	RTA	M4	17.55	4.7
17	RTA	M4	26.98	4.0
18	RTA	M4	24.74	2.9
19	RTA	M4	10.84	5.1
20	RTA	M4	25.43	1.8

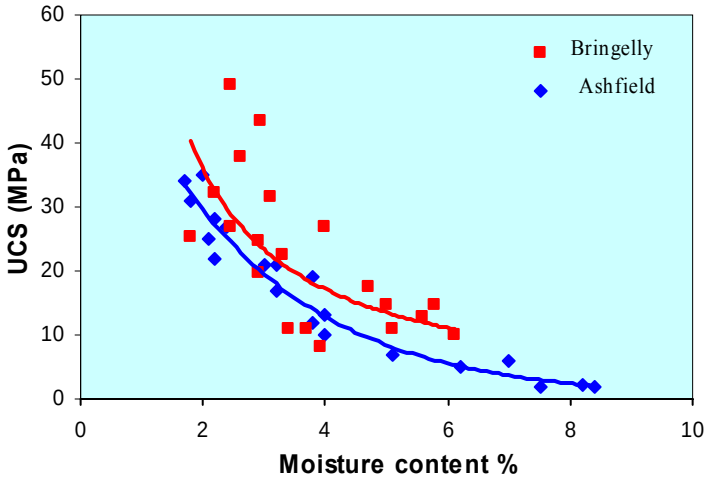

Figure 4.8 Responses of *UCS* to changes in the moisture content (data from different resources)

limited. This may have the result that only the more comptent material is tested and the typical strength is over-predicted

Although the curve from Bringelly shale agrees with the general trend, there is more scatter in the data than for Ashfield shale and the correlation has little predictive ability. Thus equation (4.5) represents a general connection between strength and natural water content, but it does not provide an indirect or convenient means of estimating *UCS* as has been claimed for Ashfield shale (Ghafoori, 1995). As all tested samples of Bringelly shale were from similar depths, it suggests that the difference in degree of saturation and mineralogy between Bringelly and Ashfield shale are responsible for the greater scattering of the Bringelly data points.

§4.3.2 **Point load test**

To further investigate the strength of Bringelly shale, axial and diametral point load tests were performed. The main objective of these laboratory tests was to investigate the effect of geometry and loading configuration on the point load strength index, and to determine the strength anisotropy of the rock. The tests will also enable an establishment of strength classification and a correlation between point load tests and uniaxial compression tests.

§4.3.2.1 **Sample preparation and procedures**

The point load tests were performed on fresh core specimens of about 51 *mm* diameter from the Kemps Creek site. Samples were tested in two directions, parallel (diametral) and perpendicular to the laminations (axial). Two series of tests were performed, the first involved specimens that tested only axially, the second involved specimens that were tested diametrally first, then the split part of the specimen with suitable size was tested axially. In all diametral tests, core samples with a length to diameter ratio greater than 1 were selected for testing. In the axial tests, core samples with a length to diameter ratio between 0.6 and 1 were used for testing. Suitably sized core samples for axial and diametral point load tests were obtained by diamond saw cutting.

A portable point load test apparatus provided by *Douglas Partners Pty Ltd*. was used. The apparatus is made of high strength anodized-aluminum and incorporates a digital display that continuously monitors applied load. The maximum load is automatically stored and easily obtainable by pressing a button. The system has a pressure sensor that is capable of measuring loads with a high degree of accuracy (Resolution = 10*N)*. The point load apparatus (Fig. 4.9) is light and has a capacity of 100 *kN* (10 *tons*).

The sample preparation and the testing procedures used for point load testing followed the suggested methods of the *International Society for Rock Mechanics* (1985). Each sample of Bringelly shale was placed into the testing apparatus such that laminations were either parallel or perpendicular to the loading axis. The calculation procedures are as follow:

$$I_s = \frac{P}{D_e^{\,2}} \qquad (4.7)$$

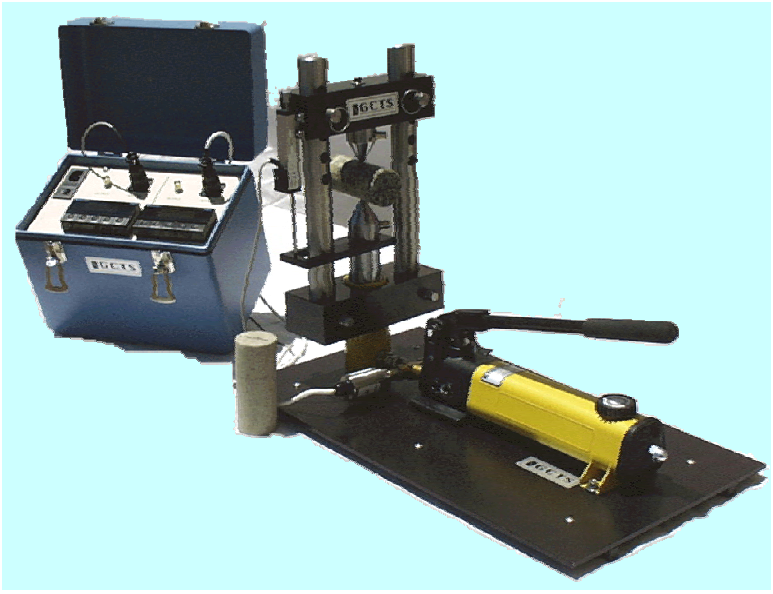

Figure 4.9
The GCTS Point Load Test apparatus

where I_s is the uncorrected point load strength index, P is the failure load, D is the core diameter, and D_e the equivalent core diameter given by:

$$D_e^2 = D^2 \qquad \textit{for diametral tests,} \text{ and} \qquad (4.8)$$

$$D_e^2 = \frac{4A}{\pi} \qquad \textit{for axial tests,} \qquad (4.9)$$

where $A = L \times D$ and L is the distance between the loading cones in an axial test.

§4.3.2.2. **Size correction**

Strength values calculated from the test have been found to decrease when progressively larger specimens are tested. However, the size and shape effects in point load testing are independent of the degree of anisotropy and loading direction (Germinger, 1982). As suggested by Broch and Franklin (1972) and further by the International Society for Rock Mechanics (1985), the results have been corrected to a standard diameter of 50 mm. This is necessary when

point load strengths are used for strength classification purpose and also for comparative studies. In this study the following equation has been used as suggested by ISRM (1985) procedure for the size correction:

$$I_{s(50)} = \left(\frac{D_e}{50}\right)^{0.50} \times I_s \qquad (4.10)$$

where D_e is measured in *mm.*

§4.3.2.3 **Test results (axial and diametral)**

Results of point load tests are usually expressed in terms of the point load strength index I_s which is, in accordance with the standards cited above. The index for a given size core is directly related to the material's tensile strength and can be correlated with UCS. Axial and diametral point load tests were performed on fresh core specimens from the Kemps Creek site. The axial point load results from specimens that were not subjected to diametral tests prior to the axial tests are shown in Table 4.5, varied between a maximum of 2.86 MPa and a minimum of 1.0 MPa with a mean value of 1.74 MPa for all samples. The standard deviation of all these samples was calculated to be 0.58 MPa.

Table 4.5 Influence of length to diameter ratio (*L/D*) on the axial point load strength.

Speciemn No.	*L/D*	$I_{sa(50)}$ (*MPa*)
KCa1	0.90	1.01
KCa2	0.85	1.00
KCa3	0.84	1.02
KCa4	0.83	1.22
KCa5	0.83	1.07
KCa6	0.83	1.08
KCa7	0.81	1.49
KCa8	0.81	1.20
KCa9	0.71	2.86
KCa10	0.78	1.53
KCa11	0.78	1.89
KCa12	0.77	1.61
KCa13	0.73	1.47
KCa14	0.69	2.63
KCa15	0.69	1.54
KCa16	0.68	1.27
KCa17	0.68	2.23
KCa18	0.66	0.97
KCa19	0.64	1.57
KCa20	0.62	1.51

$I_{sa(50)}$: diametral load test

Diametral load tests were performed parallel to the lamination planes causing the core samples to split in their weakest direction. The results have shown that diametral point load varied between 1.28 *MPa* and 0.16 *MPa*. The mean diametral point load strength of all these samples was calculated to be 0.63 *MPa* with a standard deviation of0.31 *MPa*. Other authors (Tsidzi, 1989 and Smith, 1997) have suggested that the size correction for the axial point load test is unreliable, particularly if specimens are short, and they recommended using a constant *L/D* ratio. In these tests a minimum $L/D = 0.6$ was used and *L/D* varied over a small range. The effect of *L/D* on the axial point load strength is shown in Figure 4.10. The trend line shows the point load strength reducing as *L/D* increases. All the specimens had similar water contents and would have been expected to have similar strengths, but considerable scatter is evident and the correlation is poor.

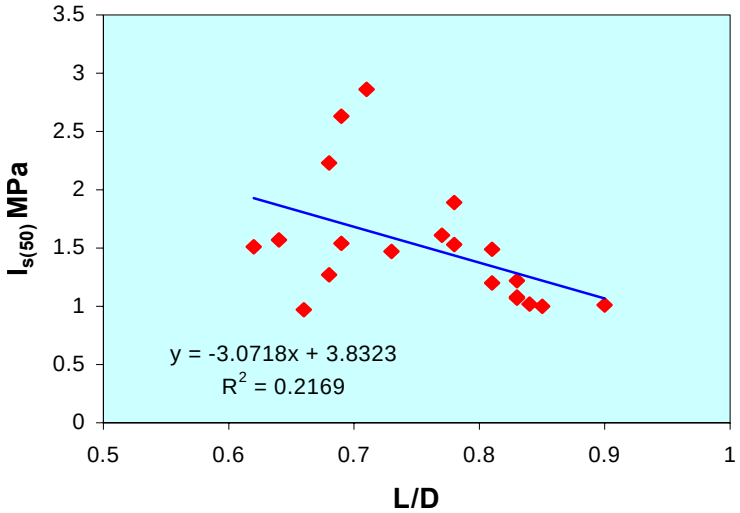

Figure 4.10 Correlation between (*L/D*) and the strength of axial point load

Similar tests on Ashfield shale reported by Ghafoori (1995) showed a clear trend of I_s reducing as *L/D* increased, and indicated a high correlation coefficient. From these

observations it is clear that the size correlation for axial point load tests is not successful in producing a unique strength index, and that the greater variability in the axial strength index can be related to variations in microcracking and degree of saturation in the Bringelly shale which are absent in Ashfield shale.

As was suggested by Broch and Franklin (1972), strength anisotropy was estimated using the term anisotropy index I_a where,

$$I_a = \frac{I_s(axial)}{I_s(diametral)} \qquad (4.11)$$

Results of the point load tests conducted parallel and perpendicular to laminations were used to measure the strength anisotropy index of Bringelly shale. A summary of the results of representative specimens where diametral and axial tests were carried on the specimen is presented in Table 4.6**.** The table shows that the values of point load strength for samples tested perpendicular to laminations were greater than those measured parallel to laminations. It also shows that the strength anisotropy index, ranges from 0.78 to 6.0 with a mean strength anisotropy index of 3.0 and standard deviation of 1.4 although 90% of values fall between 0.78 and 4.03.

The relatively high strength anisotropy of Bringelly shale can be explained by the influence of the presence of the structural micro-cracks in the plane of the laminations. These micro-cracks are believed to be the result of the history of deposition and subsequent stress relief. They may also be the result of the high concentration of K and Na (as indicated by XRD and SEM) in the clay mineralogy of the shale. These monovalent exchangeable cations are capable of causing internal swelling that could initiate structural micro-cracks in the plane of the laminations, and hence lead to the increase in the degree of anisotropy. Ashfield shale although highly laminated, does not contain similar micro-cracks and / or swelling clays. This may explain the low average strength anisotropy (Ghafoori, 1993) of Ashfield shale (I_a=1.5) compared to that of

Bringelly shale (I_a = 3.0). Based on the point load strength classification scheme suggested by the International Society of Rock Mechanics (1972), intact Bringelly shale may be described as a strong rock.

Table 4.6 Strength parameters of the load index for Bringelly shale

Specimen No.	**axial** $I_{sa(50)}$ ***(MPa)***	**diametral** $I_{sd(50)}$ ***(MPa)***	I_a
KC1	1.01	0.39	2.59
KC2	1.27	0.47	2.70
KC3	2.21	0.62	3.56
KC4	1.47	0.61	2.41
KC5	2.12	0.71	2.99
KC6	1	1.28	0.78
KC7	2.24	0.89	2.52
KC8	1.22	0.73	1.67
KC9	1.07	0.53	2.02
KC10	2.63	1.13	2.33
KC11	1.38	0.41	3.37
KC12	2.25	1.15	1.96
KC13	2.86	0.54	5.30
KC14	1.51	0.93	1.62
KC15	2.75	0.57	4.82
KC16	1.97	0.87	2.26
KC17	1.57	0.39	4.03
KC18	1.75	0.29	6.03
KC19	2.43	0.43	5.65
KC20	2.27	0.68	3.34

$I_{sa\ (50)}$: axial load strength

§4.3.2.4 **Point load testing and conversion factor**

The older literature available dealing with point load testing suggests a factor of 24 to convert axial point load strength to unconfined compressive strength (Bieniawski, 1974), while in more recent literature this value has been questioned (Quinta,1993; Smith, 1997). In this section, a comparison of the results of the point load tests with those of uniaxial compression tests on Bringelly shale will be discussed. Data provided by the *RTA* (construction of Philip Parkway Rd, Blacktown), *Coffey Partners* (Badgerys Creek Airport, Badgerys Creek), and *J&K Pty Ltd*. (Proposed Warehouse, Eastern Creek) also are included in Table 4.7. Correlations have been made between the axial point load strength and the corresponding values measured from the uniaxial compressive strength tests. The data shown in Figure 4.11 (from different sources) indicate a straight line relationship with a mean correlation factor of 21. Regression analysis shows that the correlation coefficient is 0.95.

The high correlation coefficient is surprising given the apparent variability of Bringelly shale and differences in *L/D.* This correlation factor of 21 agrees with results obtained by Romana (1995) during his comprehensive studies on different types of sedimentary rocks. A similar result was also obtained by Ghafoori (1994) who reported a correlation factor of 24.1 as the best fit relation for Ashfield shale. However, it is worth mentioning here that due to financial and time factors, there is a widespread practice particularly in the industry to rely on point load index tests rather than performing *UCS* tests. These tests can be related to a *UCS* value on the basis of an empirical correlation. For instance, comparisons between the *UCS* strength and the axial point load index (Figure 4.12) of the two shale members may indicate a similarity in their strength however, it should be noted that the data for Bringelly shale is very limited and may be being biased towards more cemented material (Section 4.3.1)

Table 4.7 Results of point load index and unconfined compressive strength tests on Bringelly shale (different sources).

Speciemn No.	$I_{sa(50)}$ (*MPa*)	*UCS* (*MPa*)
KC1	1.47	31.59
KC2	1.07	19.82
KC3	0.97	23.15
KC4	2.12	43.34
KC5	2.25	49.12
KC6	1.75	37.76
KC7	1.22	26.85
RTA	1.12	22.63
RTA	1.6	32.29
RTA	0.55	16.34
RTA	1.41	14.58
RTA	1.6	26.98
RTA	1.25	29.32
RTA	0.96	19.21
J&K1	0.45	10.0
J&K2	0,36	8.00
J&K3	0.56	12.0
J&K4	0.28	6.00
Coffy1	2.36	50.90
Coffy2	1.92	45.19
Coffy3	4.32	88.20
Coffy4	0.78	16.50
Coffy5	0.99	23.53
Coffy6	2.44	51.30

$I_{sd(50)}$: diametral load strength

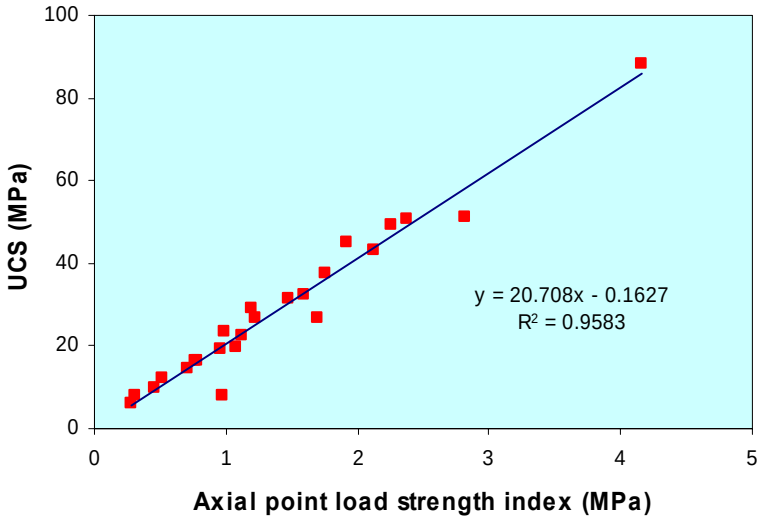

Figure 4.11 *UCS* versus axial point load strength index

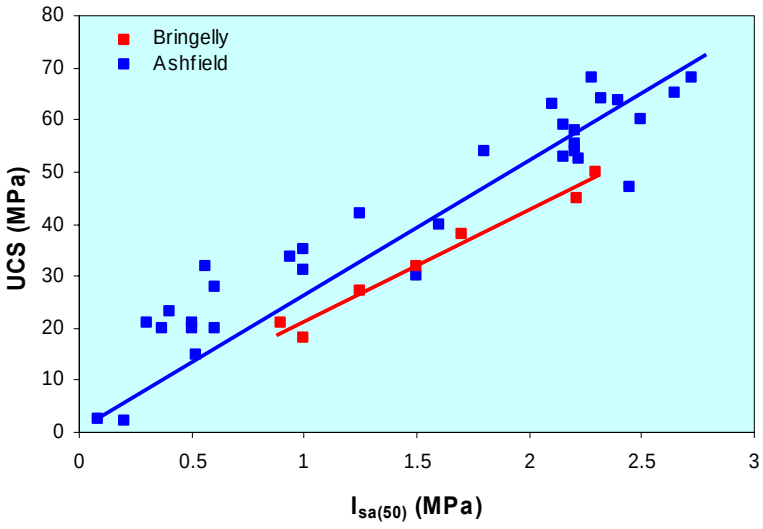

Figure 4.12 Comparison between the strength of Bringelly and Ashfield shales

§4.3.3 **Testing for susceptibility to slaking**

The durability of the shale was tested at all sites. The purpose of these tests was to establish any significant differences in the durability of shale at these sites, to investigate correlations with other properties and to develop an engineering classification. Tests have been performed on shale samples to study the interaction between the shale and water. A device shown in Figure 4.13 similar to that developed by Franklin and Chandra (1972) was used to perform slake durability tests. The method suggested by ISRM (1972) was adopted for this series. The slake durability test of Franklin and Chandra is performed by rotating six 40 to 60 gram samples in a wire mesh drum, which is partly immersed in water. The weight percentage of material remaining in the drum after two cycles (each cycle is 200 revolutions in ten minutes) defines the "slake durability index". The durability of Bringelly shale was assessed according to the value measured from the second cycle slake durability index I_{d2} as proposed by Gamble (1971). However, the tests were continued for four cycles of slaking, and the results are discussed in the following section.

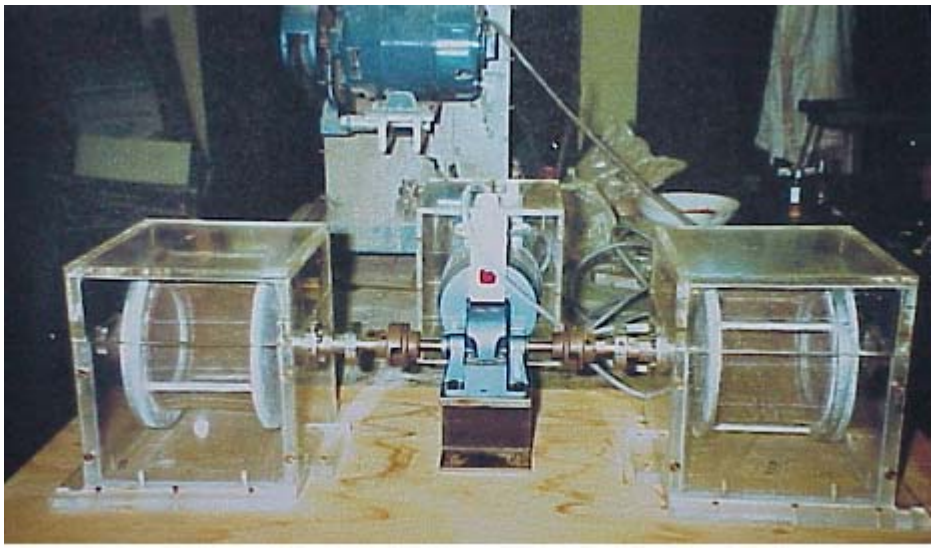

Figure 4.13 Slake durability testing apparatus

§4.3.3.1 **Slake durability test results**

Tests were performed on sixty four samples of Bringelly shale. From each site, samples were selected to represent states of weathering from fresh to extremely weathered. To investigate the effect of slaking on fresh samples, sixteen sub-samples of fresh Bringelly shale specimens from the four sites were tested. The average test results, shown in Table 4.8, revealed that the durability of Bringelly shale is not constant but varies slightly from one site to another. Slight variation was also detected between fresh samples at one site.

Table 4.8 Average durability of fresh Bringelly shale from the four sites after two slaking cycles

Site name	Number of slaking cycles	
	Id_1	Id_2
KC	80.7	66.7
BC	84.8	61.91
HP	81.72	63.5
ML	83.5	61.0

This was not surprising as the previous sections have shown variations in porosity and water content of fresh shale between the sites as well as within each site. Moreover, the definition of the various grades of weathering was subjective depending on personal observation and visual assessment. However, the data shows an acceptable degree of consistency as demonstrated by the influence of weathering on the second slaking cycle (Fig.4.14).

In order to investigate the effects of number of cycles on the durability of Bringelly shale, tests were performed on eight representative samples from the Badgerys Creek Site at pre-determined degrees of weathering. In these tests a constant slaking time of ten

minutes was used in each cycle. The durability indices after each of the four cycles are summarized in Table 4.9. The data support the suggestion of Gamble (1971) that two ten

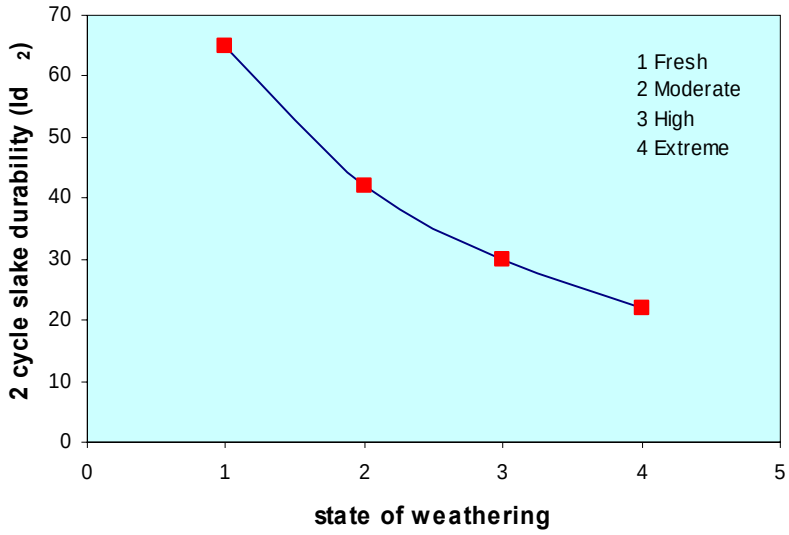

Figure 4.14 Effect of weathering on 2 cycle slake-durability (% retained) for Bringelly shale

Table 4.9 Influence of number of cycles on the durability of Bringelly shale from the Badgerys creek site

State of weathering	Slake durability index (%retained)			
	Number of cycles			
	1	2	3	4
Fresh	81.09	64.35	52.15	48.6
	79.88	62.91	53.79	50.5
Moderately weathered	71.6	43.5	31.2	23.6
	69.93	45.82	33.64	26.3
Highly weathered	59.3	28.67	20.06	16.09
	55.8	31.06	18.5	13.96
Extremely weathered	33.32	21.72	15.61	13.86
	39.19	20.31	15.01	12.94

minutes cycles give a reasonable distinction between the samples. Selected data points were further used to demonstrate the influence of increasing number of cycles of wetting and drying on the durability of the Bringelly rocks at that site. The line graph representing these data points (Fig. 4.15) shows that the percentage retained decreases with the number of cycles of wetting and drying.

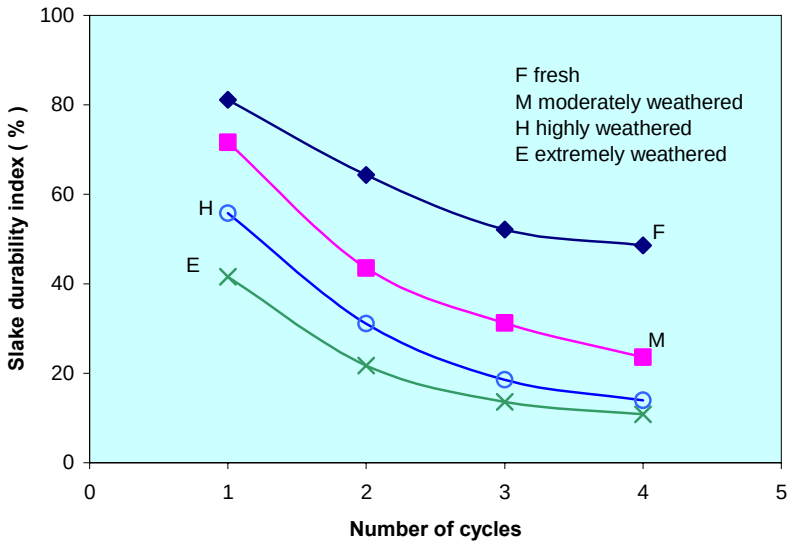

Figure 4.15 Effect of number of cycle on the slake durability index for different states of weathering

The classification scheme suggested by Gamble (1971) and Franklin and Chandra (1972) was adopted to assess the durability of Bringelly shale. Based on the test results, the durability of Bringelly shale varies from medium for fresh intact shale to very low for extremely weathered shale. The current results indicate consistency in durability among all sites. However, the variation in durability between samples with different degree of weathering at all sites is believed to be consistent with the increase of mixed-layer clay minerals and smectite as the material degrades from fresh to extremely weathered (Chapter 3). The similar durabilities for the shale with a particular grade of weathering suggest that durability is primarily controlled by mineralogy. Differences in structure (micro-cracking and cementation) would be expected within and between sites but these have apparently had little influence on durability.

The purpose of any engineering classification scheme is to provide terms that aid the user in distinguishing between materials which have similar engineering properties. The recent classification schemes for argillaceous materials have attempted to account for the important role of durability by including slaking factors. However, these schemes failed to recognize the influence of environmental factors such as temperature and humidity on the disintegration of shales, especially those with expandable clay minerals. However, these schemes have considered the influence of the non-expandable clay minerals on the durability of shales. This was evident from the difference in durability between Ashfield and Bringelly shales. Ashfield shale is more durable than Bringelly shale due to the absence of the swelling clay minerals in the first and their presence in the latter.

§4.3.3.2 **Influence of Atterberg limits on slake durability**

A relationship between slake durability and liquid limit was initially suggested by Gamble (1971) as a useful method by which weak rocks could be classified for engineering purposes. This was demonstrated for Bringelly shale by plotting the relationship between index of slake durability and the liquid limit in Figure 4.16. The tests were performed on samples showing different states of weathering. The effect of increasing number of cycles of wetting and drying is also shown in Figure 4.16. The Figure shows a clear correlation between the slake durability index and the liquid limit

for Bringelly shale. The increase in liquid limit is associated with a reduction in slake durability. This also agrees with the previous results (Section 4.2.3) that showed an increase in liquid limit and plasticity index as the material is subjected to more weathering. These results may provide more support to a better argument that it is the mineralogy and not the fabric or cement that may control the durability of Bringelly shale.

Due to the significance of liquid limit on the strength of the material, Morgenstern and Eigenbrod (1974) have established a classification scheme that could assess the amount of slaking according to the range of their liquid limits. In this study, liquid limit was used

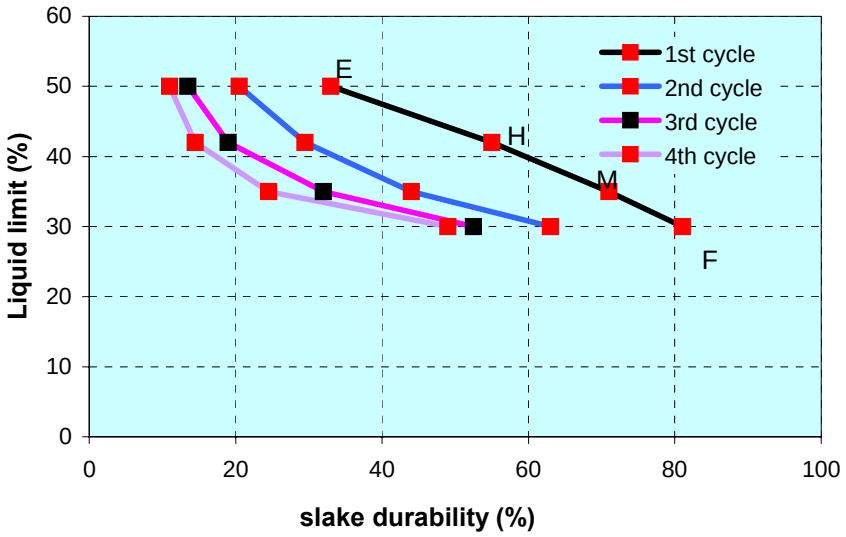

Figure 4.16 Influence of state of weathering on the relationship between liquid limit and the index of durability at various cycles

to investigate the durability of the shale based on its weathering state and the number of cycles during the test. The test results were agreeable with the classification scheme of the above authors in that the lower the liquid limit the lower the slaking.

Based on the relationship between liquid limit and plasticity index of Bringelly shale (Section 4.2.4), it can be inferred that the increase in slake durability index is also associated with a decrease in the plasticity index of Bringelly shale. Following the durability-plasticity classification scheme that was proposed by Gamble (1971), Bringelly shale would range from a medium durability-low plasticity fresh shale to a very low durability-medium plasticity extremely weathered shale..

§4.3.3.3 **Influence of state of weathering on the durability of Bringelly shale**

Durability tests were conducted on Bringelly shale from all sites with different state of weathering. The relationship between weathering and slake durability index shows that the percentage of the samples retained decreases steadily as the rock is more weathered. The data show a correlation exists between states of weathering and durability of the rock. It has been shown previously that a correlation between water content and states of weathering has been established. However, because of variations in degree of saturation this may not be a reliable indicator. Porosity or dry density would provide a more reliable indicator of weathering, but these are difficult to measure accurately. In the field, for this type of shale it was rather difficult to visually distinguish between slightly weathered and moderately weathered material. The term moderately weathered used in this study has also covered slightly weathered material. Due to the subjective definition of weathering, it is recommended that assessment of durability should be based on more than one measurement of water content, porosity, mineralogy, and Atterberg limits.

§4.3.3.4 **Assessment of Bringelly shale in relation to slake durability**

The clay shale used in this study can be defined as a sensitive ”clay shale” rock that is characterized by a high strength when in-situ, but sensitive to water chemistry changes. Reactivity to water particularly in unconfined conditions is often caused by absorption within the interlayers of the clay mineral structure. With unconfined clay shale chunks, like those used in slake durability tests, the disruption of bonds due to the immersion, or wetting and drying cycles, can act to break apart the specimen. In engineering terms, this

may indicate that Bringelly shale is a rock that can undergo significant deterioration of its mechanical and physical properties as a result of interactions with water. This definition recognizes that the term "clay shale" implies a transitional material rather than a material with well-defined initial properties. It can be seen that the slake durability test is normally used to distinguish durable and non-durable shales. However, additional tests for durability are sometimes necessary. In this study, further investigations to the mechanisms responsible for the slaking of shales were conducted by performing tests to assess the free swell potential and the influence of pore fluid chemistry on the swelling of the shale. These tests and mechanisms are discussed in the next section.

§4.3.4 **Testing the pore water suction in Bringelly shale**

The laboratory tests performed on Bringelly shale has shown that the material has a low porosity between 5% and 12% and unconfined compressive strength of between 10 *MPa* and 50 *MPa*. The reason for these high *UCS* value is believed to be partially or may be totally due to a combination effects of the fabric and pore water suction of the material. This was evident as small lumps disintegrate rapidly when placed in water. It has also been reported that the attempts to saturate the shale at low effective stress can lead to partial disintegration of the specimen (Itakura, 1999). It thus appears that the strength of the rock is largely derived from pore water suctions in its natural state. In the current study, the significance of pore water suctions was evident from the high values of stiffness measured for Bringelly shale at its natural moisture and at low confining stress (Section 5.4.9).

The force of suction is primarily dependent on the particle size distribution of the material (Delage et al. 1998). Water suction is defined as the potential energy of water per unit mass of water in the system (Gee et al., 1992). In the context of this study, it is more appropriate to consider pore water suction as a function of the hydrostatic or pneumatic pressure acting on the water. Quantitatively, it is the difference in ambient

pressure and the pressure generated by the water content of the material (Ridley, et al., 1993).

§4.3.4.1 **Apparatus and results**

The water suction characteristic of natural Bringelly was measured using a *WP4 Dew point potentiameter*. The chilled mirror psychrometer device is capable of measuring suction with a resolution of $\pm 0.01 MPa$ (Figure 4.17). Suction tests were performed on specimens from Bringelly shale and also on two specimens from Ashfield shale that were obtained from *West Ryde* (R1) and *Homebush* (H1), *NSW*, by permission from *Douglas*

Figure 4.17 A Wp4-T Dewpoint PotentiaMeter (left) and a temperature control device (right)

Partners Pty Ltd and are believed to be fully saturated. A water content of a portion from each specimen was measured prior to the commencement of the test. The remainder of each specimen was tested in the above device at their natural water contents.

The aim of performing the tests was to investigate the influence of degree of saturation on the pore water suction of the Bringelly shale which is partially saturated. It should be noted that no attempt was made to measure the full soil characteristic curves (SWCCs) to

estimate the unsaturated hydraulic conductivity function of the Bringelly shale. The prime focus was towards the investigation of the mechanical behaviour of the shale rather than exploring the soil-water transmittant behaviour of the material. A temperature control device that ensures specimens temperature from 24-25 C^{o} is also used prior to the measuring of suction. As the test is completed, *WP4* flashes a green light and the final reading of *pF* and temperature of the specimen are displayed.

Since suction is measured in units of *pF*, the *WP4* measurement had to be converted to *MPa* so that results can be compared to other tests. The following expression was used:

$$pF = \log_{10}(MPa \times 10200) \qquad (4.12)$$

In this context, *pF* is defined as the logarithm of the negative of the water potential, with the water potential expressed as cm of H_2O. There are 10200 cm of H_2O in one *MPa*. Based on the above equation, a suction stress of 1 *MPa* is approximately *pF*4.

It is worth mentioning here that no correction was required for the temperature since the calculation to determine the readings displayed takes the sample temperature into account (Petry et al., 2002). Test results of specimens from Bringelly and Ashfield shales are shown in Table 4.10. The data show the influence of water content on the pore water suction of the material.

Table 4.10 Data from suction test on the natural Bringelly and Ashfield shales

Specimens	Suction (*MPa*)	*pF*	Temperature C^o	*Mc%*	*S%*
BC1	159.09	6.21	24.9	2.11	51
BC2	158	6.20	24.3	2.07	49
BC 3	153.81	6.24	24.3	1.92	54
KC1	155.59	6.20	24.7	2.21	69
KC2	160.04	6.21	24.4	2.04	72
R1(Ashfield)	67.75	5.80	24.7	2.30	96
H1(Ashfield)	71.30	5.85	24.6	2.07	98

Despite the small absolute variation in the water content of the specimens tested from Bringelly shale, the measurements have indicated an increase in the stiffness with the increase in the water content. The data also show a significant difference in suction stress between Bringelly and Ashfield shale as shown in the above table. Because of its fully saturated state, Ashfield shale has shown a significant reduction in the suction stresses compared to those shown by Bringelly shale. This may indicates the influence of the degree of saturation on the suction of the material and also shows the sensitivity of suction to the water content of the natural material. The significantly increased values of suction in the unsaturated Bringelly shale may explain the high *UCS* values of this material. However, the role of partial saturation in estimating the stiffness of the natural Bringelly shale will be discussed in Chapter 5.

§4.4 SWELLING OF BRINGELLY SHALE

It has been well established that swelling in shale rocks can significantly affect their physical and mechanical properties. One consequence of this swelling is that standard water flush drilling techniques can give very poor core recovery. In order to understand the fundamental mechanisms that control the swelling behaviour of Bringelly shale, experimental investigations have been conducted.

§4.4.1 **Unconfined swell test**

The main objective of the free swell tests was to measure the axial and volume strain developed when unconfined shale rock specimens are immersed in water, and to further study the influence of the specimen's size on the rate of strain and hence the total strain.

The test also aimed to investigate the influence of surface area of the specimens on the swelling strain and to further investigate the influence of geometry and size on reducing the swelling potential. The investigations have also included:

(a) mineralogical and fabric analysis, together with observations of formation of cracks described previously in Chapter 3,
(b) influence of volume and geometry on swelling strain under one ambient fluid (tap water), and
(c) short term free swelling tests under different ambient fluids.

In the following sections, results of these investigations are presented and discussed, and related to the results presented earlier regarding mineralogy and fabric.

§4.4.1.1 **Preparation and procedures**

Due to the nature of the material and its tendency to disintegrate, it was not possible to machine the specimens from Bringelly shale as suggested by the ISRM (1985) guidelines. An alternate and time consuming technique was adopted using rough dry sandpaper to slowly and accurately reform the specimen to the required geometry with an axis normal to the specimen's bedding plane (laminations). As the specimen from Ashfield shale was more resistive to disintegration, it was prepared to the right geometry using a small diamond saw (dry cut).

Specimens were prepared with different geometries including cylinders, rectangular prisms, and cubes. Among these samples, two cylindrical specimens with distinctly smaller dimensions from Kemps Creek were prepared specifically to study the effects of size on swelling behaviour. Immediately after the completion of preparation and trimming, samples were wrapped in thin plastic film to prevent further loss of moisture.

However, it is believed that the technique used and the time taken (1.5 hour) to prepare each sample may have caused a loss in the natural water contents of these samples. Twenty specimens cut from fresh block samples collected from the four locations were prepared for the free swell tests. An additional fresh core sample from Ashfield shale was also cut and prepared.

The apparatus used in these series of tests, shown in Figure 4.18a, was designed and constructed during the course of study in accordance with the ISRM specifications (1979). The apparatus, (Figure 4.18b) made of 10*mm* thick Perspex, includes a $70 \times 70 \times 50$ mm cell that contains the designated specimens and is capable of being filled

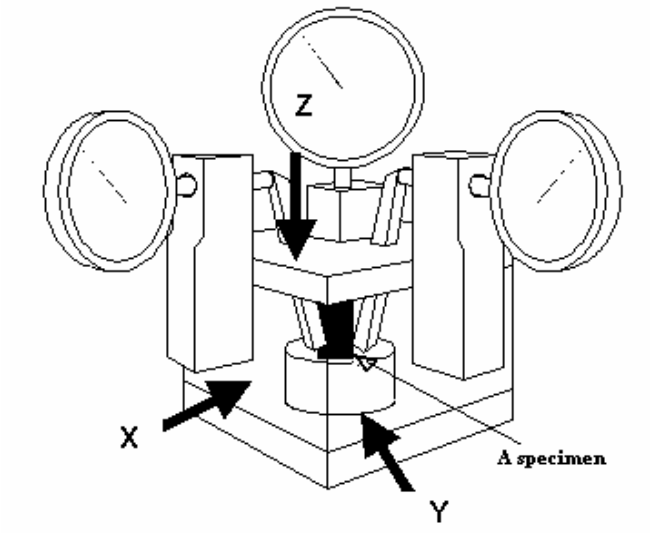

(a)

Figure 4.18a Design of the free swelling testing apparatus showing the principal axes of swelling

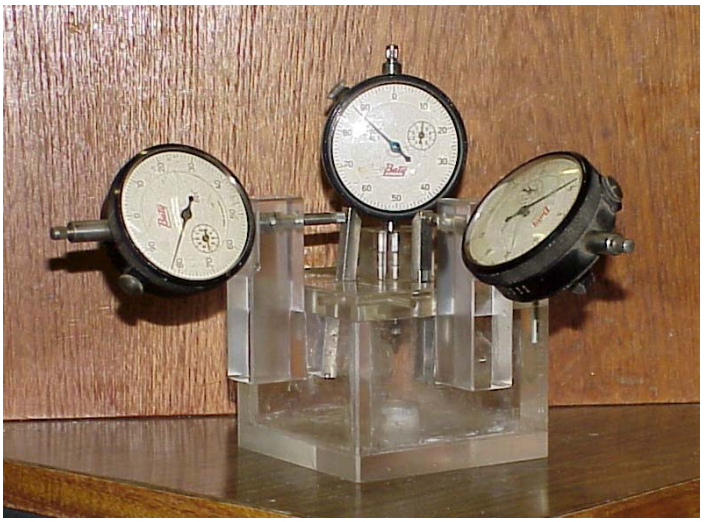

(b)

Figure 4.18b A free swelling test in progress.

with water to a level above the top of the specimens. The design allowed the use of a specimen with maximum dimensions of 30 *mm* diameter and 30 *mm* height. Different geometries can also be used within this range.

In order to perform the free swell tests, samples were placed in the apparatus with their bedding planes perpendicular to the vertical axis, and were immersed in water with various salt concentrations. The main principle of the designed device was based on the expansion of the specimen in three mutually perpendicular directions. Sensitive springs attached to the faces of the specimen for the vertical axis (z) and horizontal axes (*x*, *y*) kept the specimen in contact with the fixed dial gauges and enabled the expansion in the three axes to be measured. These gauges are capable of measuring expansion to 0.0025 *mm*. The test was carried out for a period of 36 hours during which the swelling was completely ceased. The readings were used to calculate the lateral and vertical strains of each specimen throughout the test. The volumetric strains (ε_V) for specimens with different types of geometry were then calculated using the expression:

$$\frac{V_a - V_b}{V_b} \times 100 \qquad (4.13)$$

where V_b and V_a are volumes of the sample before and after swelling

§4.4.2 **Confined swell test**

A confined swell test on a cylindrical specimen (45 *mm* diameter by 100 *mm* height) from the Badgerys Creek site was also conducted. A swell test under 600 *kPa* confining stress was performed in a conventional triaxial cell. The aim of the test was to investigate the potential swelling of the natural shale at the pressure used to saturate natural core specimens during stress path tests. This was carried out by saturating the specimen first and then relieving the stress to a nominal confining effective stress of 20 *kPa*. Measurements of axial and radial displacements were taken during saturation and during reduction of effective confining stress. In order to measure small axial and radial strains, internal and external displacement measuring devices were used. The experimental procedures and equipment used in this test were similar to those for the shear tests and are described in detail in the next chapter (Section 5.4.1). The unique feature of the swelling test was the use of internal instrumentation to measure strains during saturation. These devices are discussed in the next section.

§4.4.2.1 **Measuring devices**

Internal axial and radial deformations of the specimen were measured by using two axial and one radial Hall Effect Transducer (*HET*). The axial transducers had a range of + / - 3.5 *mm* and resolution of approximately 0.001 *mm*. The radial *HET* had a range of +/-1.5 *mm* and the resolution of approximately 0.001 *mm*. The axial transducers were glued to the rubber membrane opposite to one another along the axis of the specimen. The radial transducer was glued at the mid-height of the specimen. A fast drying instant adhesive with filler material (LOCTITE 480) was used as glue. All *HET*s were calibrated using a micrometer gauge.

An external *LVDT* transducer was also mounted on the proving ring and normal to the triaxial cell. Cell and back pressures were supplied separately by 2*MPa GDS* digital controllers. As the test was conducted under drained conditions, the volume change was measured by the back pressure controller except during saturation stage when *HET*s were used. All data have been logged automatically by a *PC* using 16 bit *A/D* plug in card. A computer program in Visual Basic was used to fully control the test. The apparatus, a schematic layout of the apparatus used, and a view of the internal devices are shown in Figures 4.19 to 4.21 respectively.

§4.4.2.2 **Test procedure**

An intact specimen from Badgerys Creek was mounted in the triaxial apparatus and 1.2 *mm* thick membrane was used to cover the specimen to separate confining fluids from pore fluids, to prevent possible leakage, and / or damage to the specimen due to cell pressure acting on the specimen. Prior to the commencement of the test, it was necessary to adjust the loading motor and the proving ring so that the axial load and the confining

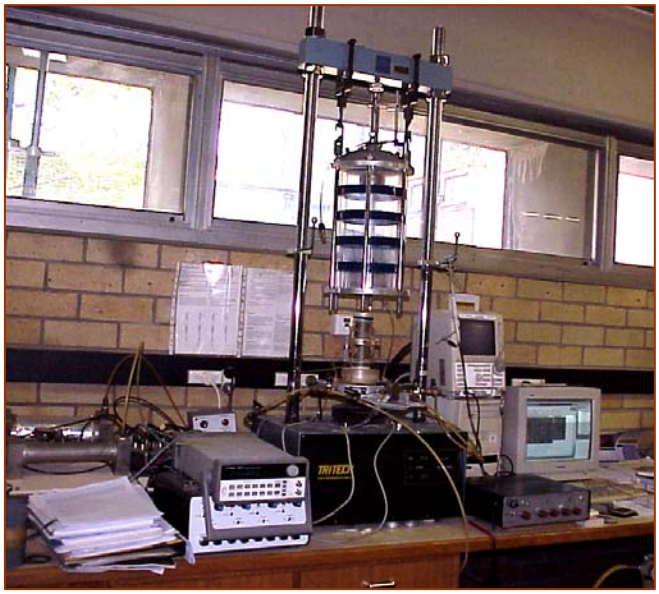

Figure 4.19 A complete set-up of the triaxial equipment

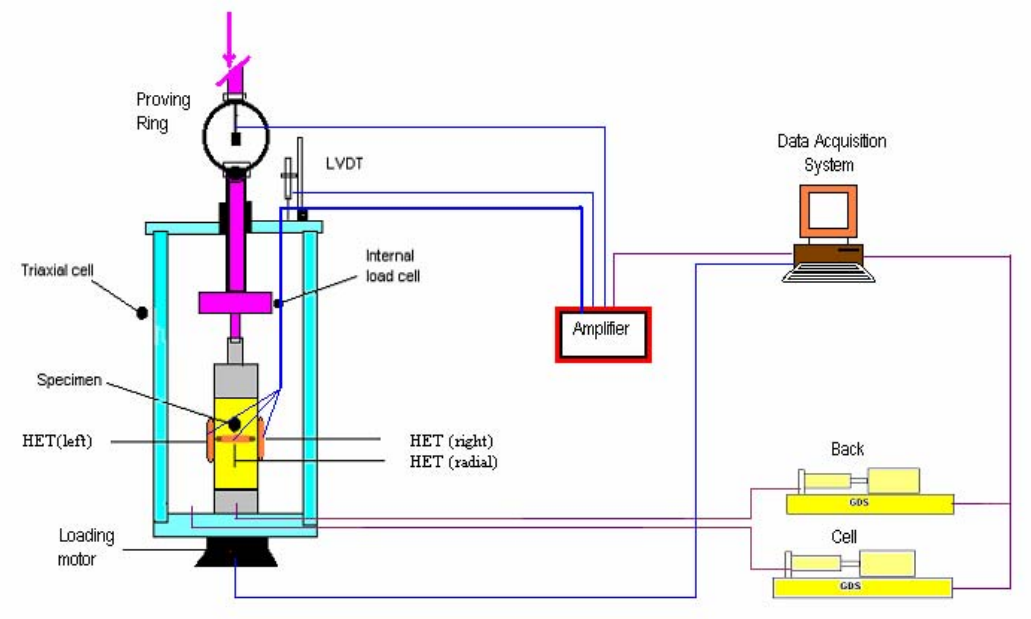

Figure 4.20 General layout of the conventional triaxial apparatus used To measure the swelling strains

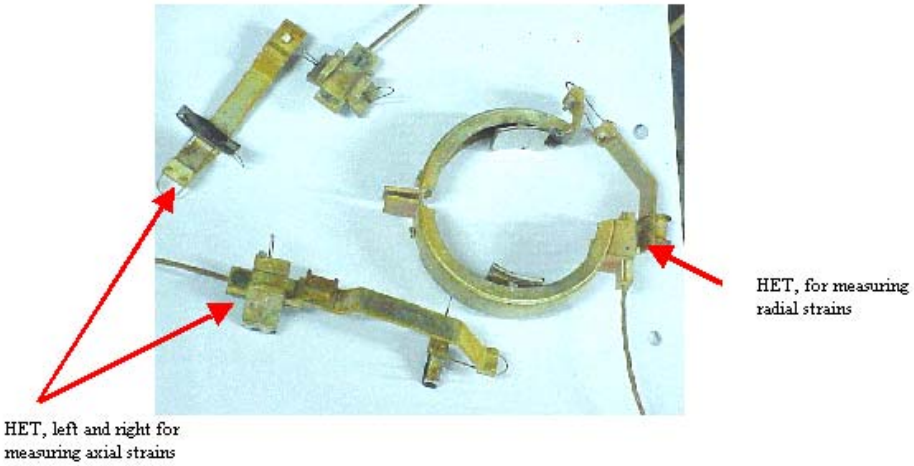

Figure 4.21 Axial and radial devices used for measuring the swelling strains

stress are the same. To saturate the specimen a back pressure of 1000 *kPa* was applied while the cell pressure was set at 1600 *kPa*, so that after saturation the mean effective stress would be 600 *kPa*. During saturation phase, air was allowed to bleed from one end of the specimen. The volume of water pumped into the specimen was reported against the volume of water pushed out of the cell. About 500 minutes of saturation time was deemed to be complete when no further water was flowing into the specimen. At this point *B*-value of 70% was measured. This was similar to the average value measured after the saturation of other triaxial specimens discussed in Chapter 5. A swelling test was initiated by gradually reducing the effective stress from 600 *kPa* to 20 *kPa* over a 5000 minutes duration. To further analyse the influence of swelling, the specimen was sheared at the reduced effective stress of 20 *kPa*.

The cell pressure was decreased at a steady rate while the back pressure was kept constant at 1000 *kPa*. Axial and diametral strains were measured using axial and radial *Hall Effect Transducer* (*HET*). Axial strain has also been calculated from an external *LVDT*. At the conclusion of the test, raw data were copied for further processing and calculations.

§4.4.3 **Results of free swell tests**

Much larger volumetric swelling strains are measured for Bringelly shale than Ashfield shale. For specimens tested in tap water, deformation ceased after a few hours until after about 36 hours the specimen lost its integrity with some clay dispersing into the water.

Typical axial and volumetric strain responses of Bringelly shale specimens during the free swell tests are shown in Figure 4.22.

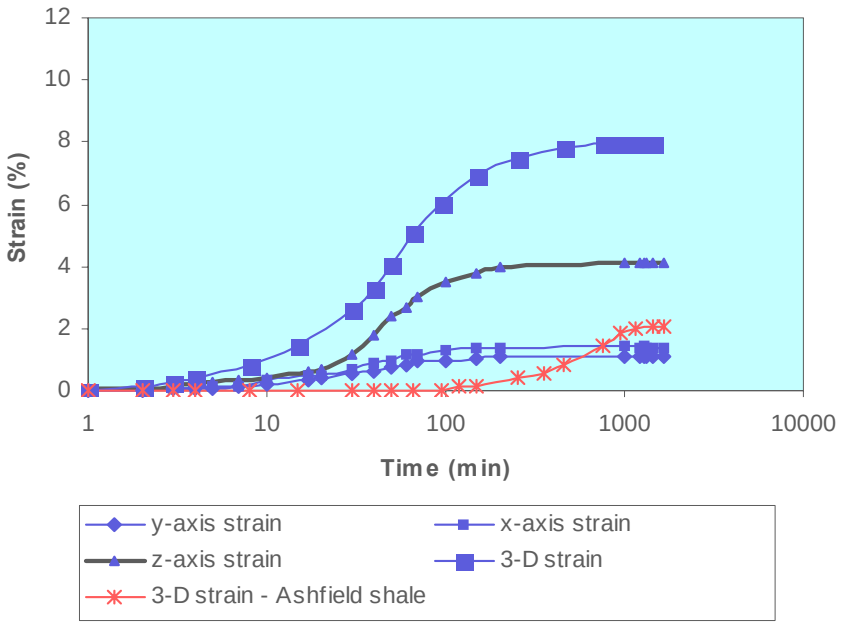

Figure 4.22 Typical axial and volumetric strain for Bringelly shale

The figure also shows the response to swelling of a specimen from Ashfield shale. For Bringelly shale, the strains are anisotropic, developing predominantly in the vertical direction. The specimens with rectangular and cube geometries had lateral strains (ε_X , ε_Y) ranging from 1.1% to 2.48 %, and vertical strain values (ε_Z) ranging from 2.8% to 4.1%. The volume strain was calculated to be in the range of 6.0% to 7.7%, with a mean value of 6.8 %.

For Ashfield shale, the strains were isotropic and small and no further deformation was monitored for a further 5 days after which the test was terminated. However, only 2000 minutes of reported data was used for analysis hence swelling was ceased afterward. At the conclusion of the test, the volume strain was calculated to be 2.15%.

Cylindrical specimens from all sites with the same initial volumes as the cube samples have exhibited lateral strains ranging from 0.96% to 1.95%, and vertical strains ranging from 2.1% to 3.9%. The volume increase was calculated to be in the range of 5.58 to 7.81% with a mean volume strain value of 7.3% and with a standard deviation of 0.63%.

Results for the three cylindrical specimens from *KC* site with different sizes were compared to a specimen with the same geometry but with a standard size. Ratio of volume to surface area for different geometry has been used to present the data (Table 4.11).

Table 4.11 Number and geometry of specimens used in the swelling test series (D.S: different sites, KC: Kemps Creek site)

Geometry of samples	Number of samples	Dimensions (mm)
Cube (Ryde)	1	30×30×30
Cube (D.S)	12	30×30×30
Rectangular prism (D.S)	2	27×25×30
Cylinder (D.S)	4	30diameter×30
Cylinder (KC)	1	22diameter×24
Cylinder (KC)	1	14diameter×26.5

The geometry, dimensions, and final volumetric strains for all specimens are presented in Tables 4.12 and 4.13. There are slight differences between the four sites, but in all cases similar responses were obtained, with greater vertical than lateral strains and significant total volume strain. The influence of different parameters such as volume, surface area, and diameter on the swelling strain of like and unlike geometry was presented in Figures 4.23 and 4.24 (further discussion in section 4.4.5).

Table 4.12 Maximum volume strains for all samples.

Site name	Geometry	Volume Strain %
Ryde(Ashfield)	Cube	2.15
HP	Cube	7.48
HP	Cube	7.29
HP	Cube	6.81
HP	Cube	7.71
HP	Cylinder	6.93
BC	Cube	6.41
BC	Cube	6.21
BC	Cylinder	5.58
BC	Rectangle	7.01
BC	Cube	6.37
ML	Cube	6.58
ML	Rectangle	6.96
ML	Cube	6.83
ML	Cube	5.98
KC	Cube	7.35
KC	Cube	7.41
KC	Cylinder	7.30
KC	Cylinder	7.81
KC	Cylinder	11.8
KC	Cylinder	15.97

Table 4.13 Influence of volume / surface area on average volume strain of different geometry

Geometry	V (mm^3)	SA (mm^2)	V/SA (mm)	ε_v%
Cube – Ashfield	27000	5400	5.00	2.15
Cube	27000	5400	5.00	6.81
Rectangular prism	20250	4470	4.53	7.01
Cylinder	21195	4239	5.00	7.3
Cylinder *	9118.6	2417.8	3.78	11.80
Cylinder *	4077.3	1472.6	2.77	15.97

NB: *V*: volume *SA*: surface area * special cutting

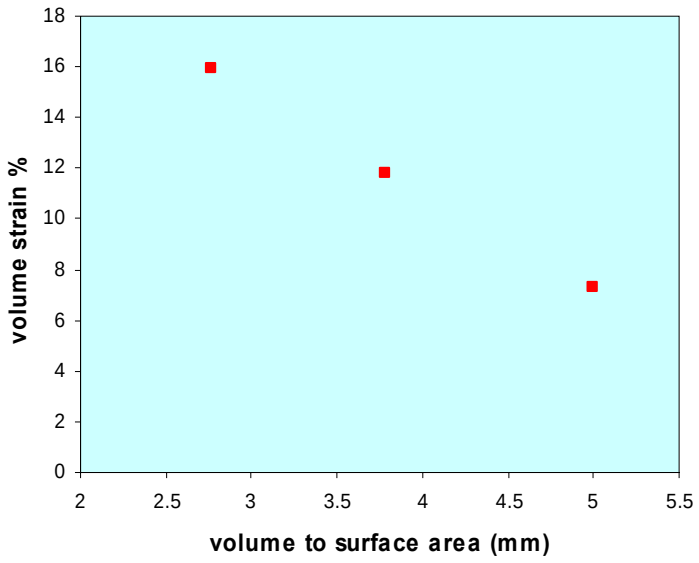

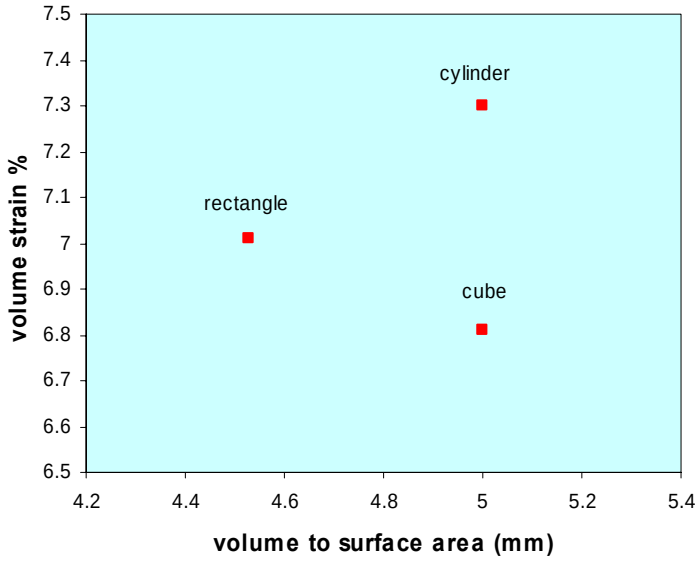

Figure 4.23 Influence of geometry (sample shape) on volume strain of cylindrical specimens

Figure 4.24 Influence of different geometry (shapes)
on volume strain of Bringelly shale

§4.4.4 **Test results of confined swell**

The objective of this test was to evaluate the effect of tap water on the axial and radial swelling strains of the natural shale under isotropic conditions. The volume of water that flowed into the specimen during the period of saturation was measured by the *GDS* and is presented in Figure 4.25. The volume of water flowing into the specimen during saturation was used to evaluate the degree of saturation of the specimen. The volumetric strain of the specimen was inferred from data obtained by the *HET*s and plotted against time (Fig. 4.26). The axial and radial strains starting from the end of saturation were also plotted against mean effective stress (Fig. 4.27). The figure shows a linear relationship with a tendency for more swelling in the axial direction. The deformation of the material during saturation to the end of shearing is illustrated in Figure 4.28. The figure shows the axial and radial deformation prior and after the commencement of relieving the pressure.

The figure also indicates 1.3% expansion in the specimen during saturation and about 4% overall swelling at the conclusion of the confining swelling test.

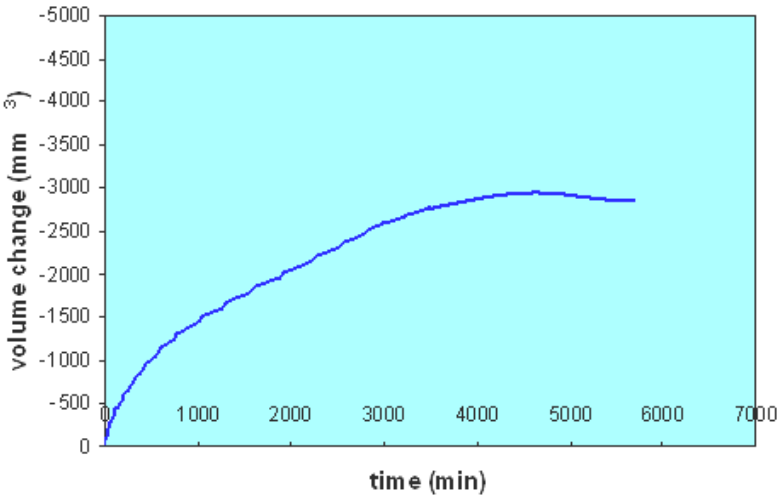

Figure 4.25 Water volume changes during saturation of natural shale (back pressure 1000kPa, confining stress 600kPa)

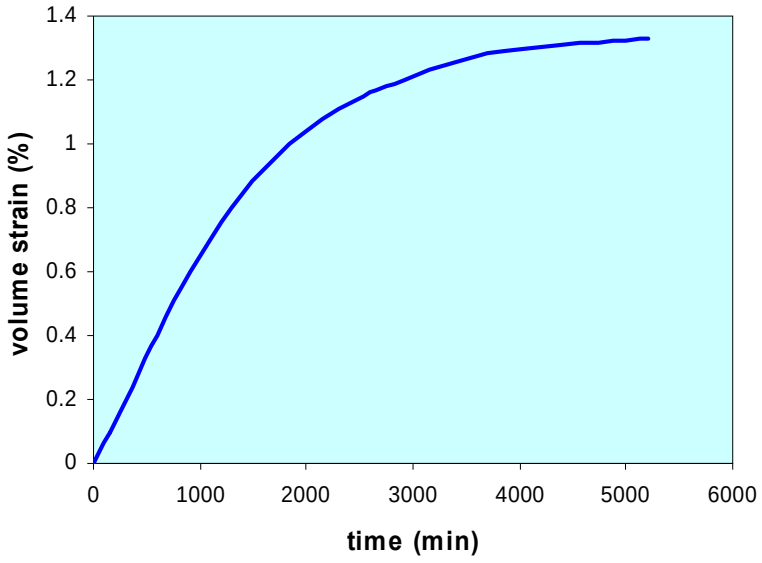

Figure 4.26 Volume strain measured from the HETs during saturation (back pressure 1000kPa, confining stress 600kPa)

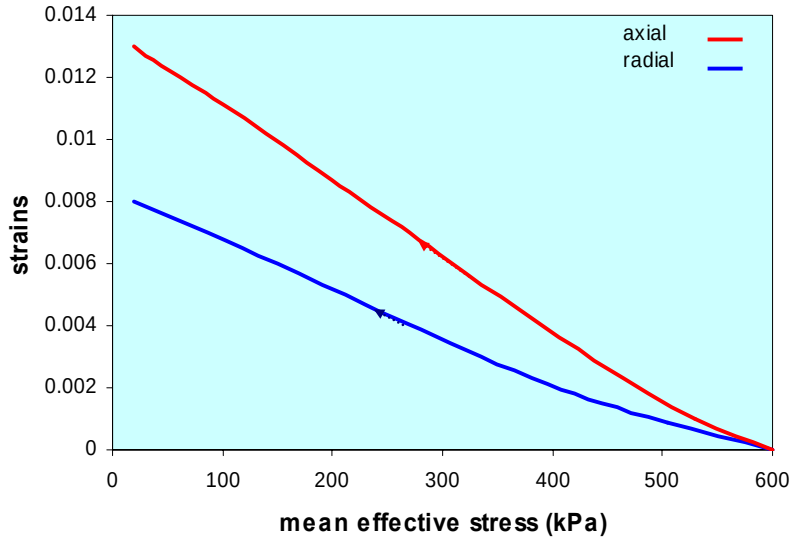

Figure 4.27 Axial and radial strain during a confined swelling test performed on a saturated specimen (confining stress reduced to 20kPa in 5000 minutes)

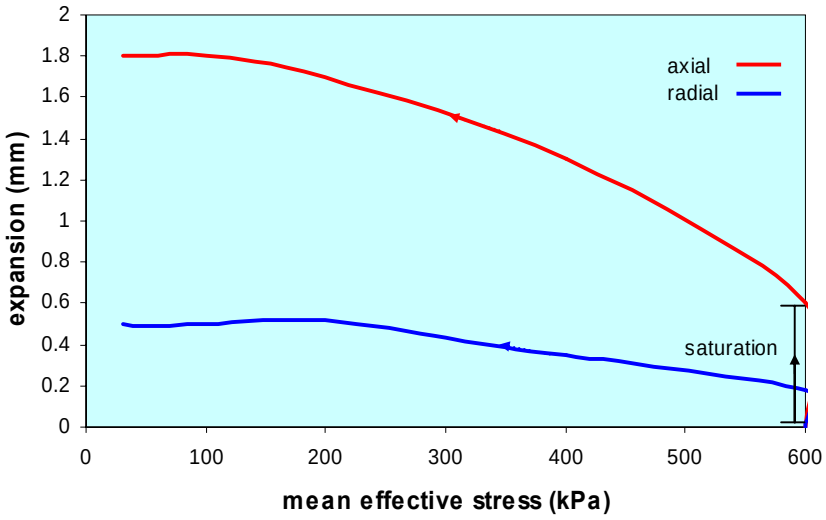

Figure 4.28 Deformation of natural Bringelly shale during subjection to swelling (arrows show direction of test)

§4.4.5 **Discussion**

To investigate the mechanisms responsible for the slaking (Section 4.3.3) of the shales further tests were performed to assess the unconfined swell potential on the swelling of the Bringelly and Ashfield shales. Further assessment involving a confined swelling test for Bringelly shale was also carried out. All the data obtained for Bringelly shale show that swelling is greatest in the z-direction, perpendicular to the approximately horizontal plane of the laminations. For the unconfined test series, $\varepsilon_z \sim 4\%$ and $\varepsilon_x \approx \varepsilon_y \sim 2\%$ (Fig.4.22) while in the confined test series $\varepsilon_z \sim 1.8\%$ and $\varepsilon_x \approx \varepsilon_y \sim 1.1\%$. In the unconfined tests, after 10 minutes, the specimens began to swell, and swelling was complete after about 5 hours. No volume changes occurred for the next 24 hours. However, after 48 hours the material was partially disaggregated with suspended fine particles observed in the swelling fluid. Depending on size and geometry, volume swelling strains of specimens varied from 4.5% to 16%.

The unconfined swelling curve of Ashfield shale exhibits different behaviour from that of Bringelly shale. The specimen only began to respond after 2 hours from the commencement of the test, the strains were equal in all directions, and volume change of the specimen stopped completely after 24 hours. A relatively small volume strain of 2.15% was measured. Moreover, after a further 72 hours immersed in water no change in the dimensions was observed, and when the specimen was removed and visually examined, no signs of disintegration were observed.

These observations can be partly explained by microcracks being present in the Bringelly specimens in the plane of the laminations, but not in the Ashfield specimens which showed uniform swelling strain in all directions. From the isotropic swelling response it would be expected for the modulus of elasticity of Ashfield shale to be the same in all directions (Wong, 1997). However, a study by Ghafoori (1994) showed that the Young's modulus of elasticity appears to be influenced by the orientation of the specimens with respect to the laminations give ratio $E_{max}/E_{min} \sim 3$.

Microscopy has shown cracks in the plane of the laminations in the Bringelly shale, the opening of these cracks can explain the preferential strain in the *z*-direction. Also cracks result in greater permeability of Bringelly shale (even though the porosity is the same as Ashfield shale) and result in more "rapid consolidation".

The unconfined swelling test results revealed that despite their uniform mineralogy, specimens exhibited variations in their swelling behaviour with changes in shape (Fig.4.24) and size. In order to explore these parameters, interrelationships between geometry, size, and strain were carefully looked into. Specimens were tested to investigate the following:

i. effects of constant volume and different geometry,
ii. effects of different volume and the same geometry;
iii. effects of the same volume and the same geometry from different sites.

Specimens with the same geometry (Fig.4.23) showed significant variation in their swelling strains, with the material swelling more as its volume reduces (Table 4.14).

Table 4.14 Influence of confining stress on the swelling behaviour of Bringelly shale

Type of test	**Geometry mode**	***V*(mm^3) range**	**ε_v% (range)**	**Average swelling%**
Unconfined	**Cubes + Cylinders**	20250-27000	6.81- 7.3	7
Unconfined	**Cylinders**	9118-21195	15.97-11.80	13
Confined (S)	**Cylinder**	159,000-161,000	1.35	1.35
Confined (AS)	**Cylinder**	161,000-157,000	2.65	2.65

The table shows the influence of the confining stress on reducing the potential of swelling. This can be noted from the average values of the volumetric strains for each test

where the swelling potential seems mostly suppressed when the material is saturated and under a constant confining stress.

The influence of geometry on the swelling of natural shale with different volumes was also investigated. It was evident from the general trend shown in Figure 4.29 that the relationship between the surface area of the specimens and their volume strain is well

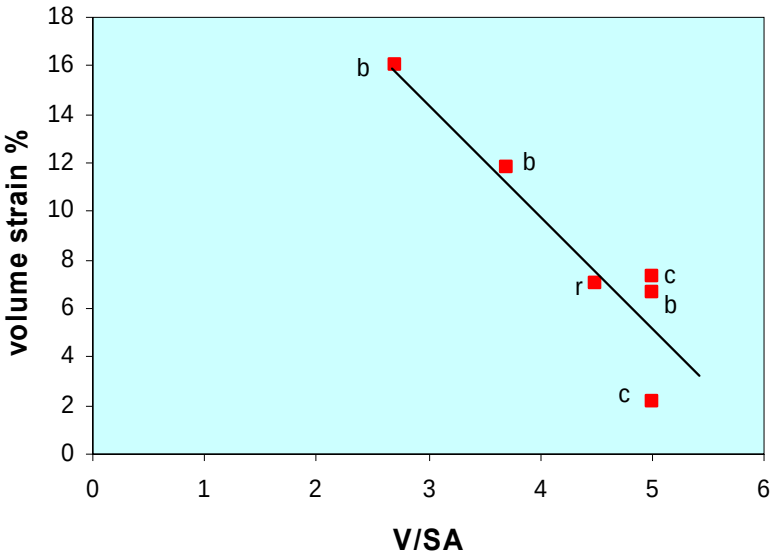

Figure 4.29 A general trend shows the influence of sample size on the volumetric strain of different geometry (b= cube, r=rectangle, c=cylinder)

maintained. The larger the specimen, the less exposure the bulk of the specimen gets to water due to its very low hydraulic conductivity and hence the lower the volume strain. However, care should be taken during the preparation of the specimens hence less equidimentional specimens may take some account of the ratio V/SA. An increase in size of the specimens is often associated with reduction in the volumetric strains.

This trend is even more pronounced among specimens having identical geometry. These observations were further investigated in an attempt to establish a numerical connection

between volume strain of the specimen (ε_v) and its diameter (d_i). It was evident that the change in the swelling of the specimen is influenced by its diameter or width. The linear relationship (Figure 4.30) is described by the following expression:

$$(\varepsilon_v) = -0.57(d_i) + 24.7 \qquad (4.14)$$

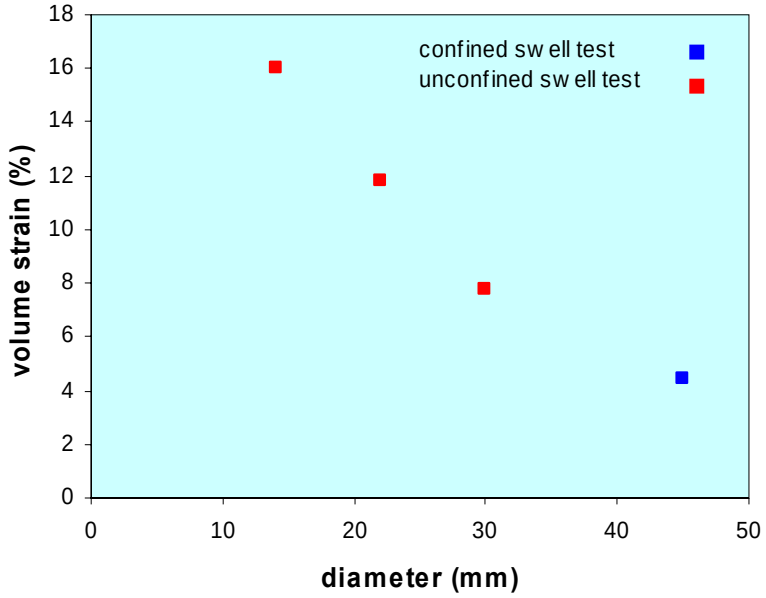

Figure 4.30 Relationship between diameter and volume strain of Bringelly shale

Regression analysis shows that the above equation fits the data with a correlation coefficient of $r^2 = 0.94$. However, caution should be exercised in the use of above equation beyond the range of the investigated specimen sizes. Extrapolation is clearly unreasonable as equation predicts compression when $d_i > 45$.

The confined swell test performed on the *BC* specimen has shown an increase in volumetric strain at two stages. The first is the stage of saturation where the specimen was saturated under 600 *kPa* confining stress. At the end of saturation, 1.35% volumetric strain has been measured. The second was the reducing of the confining stress from 600

kPa to 20 *kPa* at a constant rate. The change in axial and radial strains indicated more expansion in the axial direction than the radial and the volume strain at the conclusion of the test was about 4%. The results from the confined test show the influence of saturation in reducing the volumetric strain of the specimen, but may also imply that the reduction of effective stress acting on the material is a significant contributor in disturbing its integrity and leading the material to swell.

However, it is strongly believed that the confined volumetric strain the specimen has shown is relatively high and that yield and breakage of bond within the specimen is likely to have been occurred before shearing. Moreover, the increase in the saturation strain is also believed to be associated with a reduction in pore water suctions and hence in increasing the volumetric strain during saturation (suction will be discussed further in section 5.4.5.4).

The results of confined and unconfined swelling tests affirm the influence of confining stress in reducing the volumetric strain of the shale material and also confirm the inverse relationships between the specimen sizes and their volumetric strains at each test condition. This was evident from the 4% volumetric strain measured from a 159,000 mm^3 specimen in the confined condition, and an average of 7% volumetric strain measured from an average size of 20,000 mm^3 in an unconfined condition.

The swelling test results suggest that the influence of sample size on the swelling of Bringelly shale results from the opening up of micro-cracks during specimen preparation. If this is the case the amount of swelling in fresh shale exposed to water may be expected to depend on the excavation procedure. Much greater swelling strains are measured for Bringelly shale than Ashfield shale, and for the Bringelly shale the strains are anisotropic, developing predominantly in the vertical direction. As noted previously, opening of micro-cracks in the Bringelly shale could explain the greater vertical strains. Other possible reasons for the difference in the behaviour include swelling due to reduction in pore water suction and osmotic effects due to differences in chemistry of pore fluid and

swelling liquid. All these effects may accelerate absorption, diffusion, and the ionic exchange reaction. These possibilities will be investigated in Section 4.5.

The above may explain the physical influences such as micro-cracks, higher permeability, and suction in increasing the swelling potential of the specimens. However, the influence of other factors like surface area and geometry in increasing or decreasing the swelling potential of the shale material needs further investigations. In order to cover some of the possible physiochemical effects on swelling, pore water chemistry will be investigated and discussed in the next section.

§4.5 INTEGRITY OF BRINGELLY SHALE UNDER DIFFERENT AMBIENT FLUIDS

Drilling in Bringelly shale is costly and time consuming, and conventional diamond drilling with water flush usually results in a significant loss of core. This appears to be typical of coring operations in shale and particularly Bringelly shale. It is known in the drilling industry that shales containing swelling clay minerals can cause hole instability and considerable research has been conducted in an effort to determine suitable drilling fluids (e.g. Steiger, 1993; Lee et al. 1993; Al-Bazali, 2003). Efforts are focused particularly towards finding alternate environmentally acceptable water-based drilling fluids. The chemistry of the pore fluid is known to be important in preventing collapse. Immersion tests were performed on specimens from Kemps Creek to investigate the influence of pore fluid on the specimen integrity and hence to study the mechanisms by which the stability of the formation may be disturbed when exposed to different chemical properties.

§4.5.1 Pore fluid salinity

In order to study the influence of pore fluid chemistry on the swelling potential of Bringelly shale, it was necessary to measure the salinity of the specimens prior to the immersion tests. In order to do so, the fresh shale was pulverized and a slurry with water

to soil ratio of 1:5 prepared. The electrical conductivity of the slurry was then measured and a conversion factor for translating $EC_{1:5}$ to EC was used. An appropriate factor was used based on the ratio of soil to water and also on the clay mineral content of the soil (Charman & Murphy, 2000). Tests on specimens from *KC* were performed under the supervision of Dr John Triantafilis at the Department of Soil Sciences, the University of Sydney. The results of three specimens showed that the average salinity of the pore water from *KC* is 1760 *ppm*. This value is based on a conductivity of $EC_{1:5}$=2.7dS m^{-1}.

§4.5.1.1 **Swell test procedures**

Two series of tests were performed on fresh specimens. The first investigated the long term swelling of specimens immersed in different ambient fluids. In this series the morphological and structural changes of the specimens in each fluid were closely monitored and compared. The second series was similar to the free swell tests reported previously (Section 4.4.1) in which the deformations during swelling were recorded.

Four fresh samples from *KC* were prepared from rock cores that had been split by diametral testing. They were immersed in different fluids and visually inspected at regular intervals. The samples were 50mm in diameter and 30mm thick and were placed in four 200ml beakers filled with different fluids. The fluids and their salinities were:

1. tap water H_2O (400 *ppm*),
2. 1 molar $NaCl$ solution (58000 *ppm*),
3. 1 molar KCl solution (75000 *ppm*), and
4. 1 molar $CaCl_2$ (110000 *ppm*).

In the first test series, all samples were visually inspected before the commencement of the test. No signs of cracks or laminations were observed on the surface of these specimens. A sufficient volume of solution was used to keep the specimens submerged

throughout the test. The tests were performed in a constant temperature environment. Evaporation was minimal and the fluid concentration assumed to remain constant.

Throughout the test, all samples were visually monitored for structural changes including cracking, splitting, swelling, slaking changes in physical and morphological appearance, and disintegration. In the second test series the same preparation and procedures used in the free swell tests described previously were followed.

§4.5.1.2 **Test results**

For series 1, the first specimen immersed in tap water showed similar behaviour to that during free swelling (Section 4.4.1) and partially disintegrated after 2 days. It was also noticed that the pattern of cracking developed during the test involved incomplete horizontal hairline cracks around the circumference of the sample.

The second specimen submerged in $NaCl$ solution was monitored for twelve weeks. At the end of the first week, the specimen exhibited a few fine cracks parallel to the plane of laminations. These cracks started to get wider in size in the following weeks. After six weeks, the entire specimen showed signs of slow but minor disintegration. However, a state of equilibrium appeared to be reached as the specimen managed to maintain its shape and condition for almost three months without further deterioration.

After four weeks from the immersion of the specimen in KCl solution, close examination revealed that the specimen showed very fine discontinuous surface cracks. However, the sample managed to stay intact for almost 6 months without showing signs of swelling or widening of these early fine cracks. This is expected as potassium muds are widely used to ensure whole stability in reactive clay shales.

The specimen in the $CaCl_2$ solution showed more softening than in the $NaCl$ solution. This softening was evident from the significant displacement in the cracks that were observed two days following the submergence of the specimen in the solution. The

displacement of these cracks has resulted in a disturbance of the particle arrangement and therefore to the weakening of the cohesion between these particles. This was evident from the accumulation of fine particles around the base of the sample. The structural appearance of the samples after being recovered from the solutions is shown in Figure 4.31.

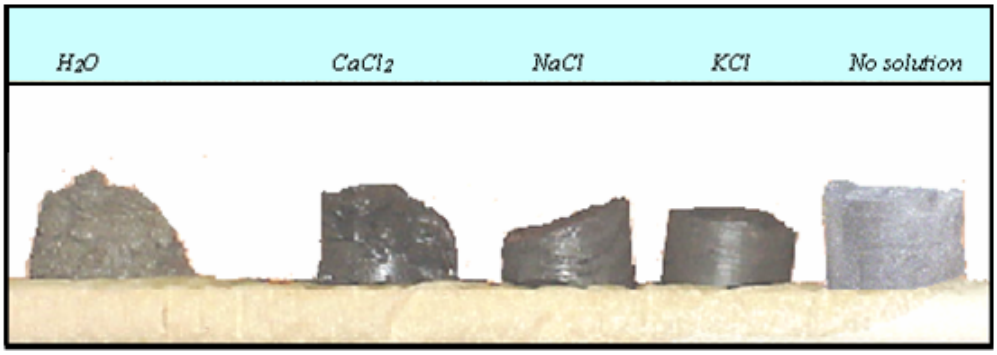

Figure 4.31 Influence of pore fluid on the integrity of Bringelly shale (visually inspected specimens)

In the free swelling test (series 2), *KCl, NaCl, $CaCl_2$* solutions, and tap water *H_2O* are used to assess the swelling potential of four cubical specimens. The results are graphically illustrated in Figure 4.32. The Figure shows that the swelling occurs in all solutions, but the volume strains increase from ~2% in *KCl* to ~8% in tap water.

§4.5.2 **Discussion**

Chenevert (1970) stated that the most important factors that lead to shale failure are that shales contain a significant amount of clay and that shales tend to hydrate when they come in contact with water. Water is also believed to be driven in and out of shale by driving forces that include hydraulic pressure, electrical and chemical potential, temperature, and concentration gradients. Shale-fluid interaction has been investigated and reviewed by many researchers (e.g. Steiger, 1993; Santos et al,1996). Previous studies of ground water from Bringelly shale (Old, 1942, PPK, 1997) have revealed that

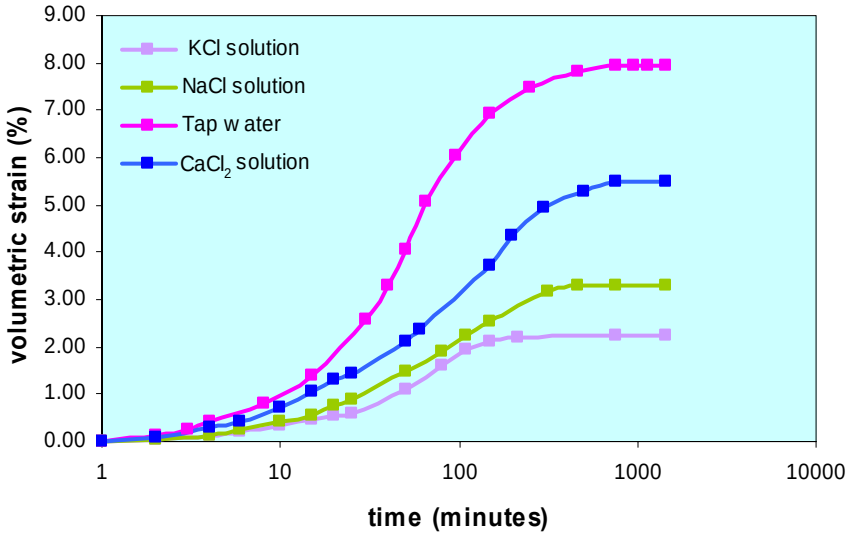

Figure 4.32 Influence of pore fluid on the swelling potential of Bringelly shale

salinity of the ground water is generally too high even for stock watering. Table 4.15 gives recorded saline content (total salt) that range up to 20500 *ppm* in the groundwater. These salt concentrations are relatively high compared to that measured in the current study.

The salinity of Bringelly rock from *KC* was determined to have an average of concentration 1760 *ppm*. The difference in salinity is believed to be due to the difference in depth of the groundwater and the depth from which the *KC* specimens were collected. In order to establish a mechanism to explain the swelling potential of Bringelly shale, the influence of pore water suction (Section 4.4.5) and the effects of the double layer were used as a basis for interpreting the test results. The double layer theory relies on the process of diffusion where ions transfer from zones of higher concentrations to zones of lower concentrations.

In a clay-water system, the reduction of chemical potential of water is a result of interaction between water and clay mineral surface. This may create a gradient in the chemical potential that may cause additional water to flow into the system.

Table 4.15. Groundwater and leachate quality results (modified from PPK,1997)

parameter	Unit	results of the laboratory analysis							
		B1	B2	B3	B4	B5	B6	B7	B8
Salinity	**Ppm**	9520	11380	20500	15400	6150	15000	5540	5790
conductivity	**uS/cm**	16650	19700	34100	26500	10990	25800	9560	10350
TDS	**Mg/l**	10500	14300	25300	20300	11400	18200	8560	6220
potassium	**Mg/l**	19	64	51	81	61	47	52	18.5
Sodium	**Mg/l**	2710	3040	5270	3850	2600	3410	2400	1460
Calcium	**Mg/l**	147	379	315	604	334	509	259	203
magnesium	**Mg/l**	481	409	1130	630	364	849	224	189
Chloride	**Mg/l**	4880	6080	11100	8540	5240	8020	4220	2570
bicarbonate	**Mg/l**	1100	859	805	740	678	680	1010	1000
Sulphate	**Mg/l**	399	ND	665	ND	26	400	ND	42
Fluoride	**Mg/l**	0.6	0.3	0.4	0.2	0.3	0.2	0.2	0.3

In the current tests, these observations were noted:

i. although volume strain was ~ 2%, upon exposure to potassium chloride, the specimen managed to maintain a high degree of integrity regardless of how long it was exposed to the solution,

ii. it gradually showed a minor change in structure when exposed to sodium chloride solution, a 3.3% volume strain was measured,

iii. a specimen immersed in calcium chloride demonstrated a relatively high swelling strain. Structural changes were observed that led to disintegration of the specimen.

iv. shale specimens immersed in tap water swell significantly, disintegrate, and gradually lose integrity with time.

Figure 4.33 shows that the increase in expansion generally follows a reduction in concentration of the solution. However, the specimen tested in $CaCl_2$ solution with the highest salt concentration has exhibited an intermediate expansion state that lies between specimens tested in H_2O and $NaCl$ solutions. This suggests that the valency, and possibly cation species are also influential.

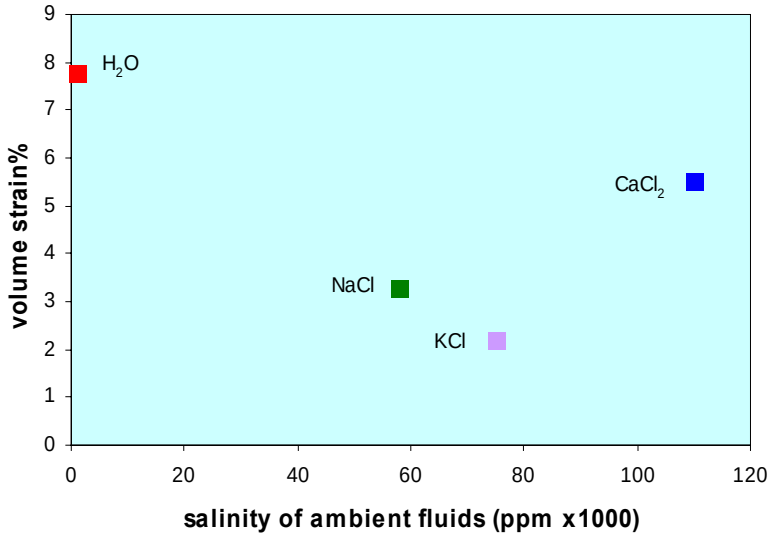

Figure 4.33 Influence of salinity of ambient solution on swelling potential of Bringelly shale

On the basis of the experimental data available it is suggested that swelling is caused by a combination of two processes, the first is the inflow of water to equilibrate pore water suctions and the second is the chemically driven processes caused by changes to "double layer" thickness. The former is a consolidation process controlled by the permeability of the shale, the latter is a diffusion process driven by differences in concentration gradient. In practice these are likely to be coupled as the water flows required for consolidation will transport the ambient fluid more rapidly into the shale specimens.

Osmosis and water hydration are thought to be the main causes of the swelling of the double layer thickness whereby the ambient water is driven into the shale specimen by differences in concentration gradient. This causes the cations in high concentration in the

pore fluid to diffuse out. The ongoing diffusion of cations lowers the concentration and reduces the ionic strength of the specimen. This leads to an increase in the repulsive force and hence to subsequent increase in the inter-particle spacing. This eventually will cause expansion to the whole specimen. This was evident from data given in Table 4.15 that indicated a low concentration of potassium ions compared to that of calcium, sodium, magnesium, aluminum, and chloride.

Since KCl, $NaCl$, and $CaCl_2$ solutions were more concentrated than the initial pore fluid of the specimens, double layer changes may be the most likely mechanism. It is believed that ion movement due to difference in concentration between the specimen and the ambient fluid is eventually bringing the system to a state of equilibrium. This state can eliminate the osmotic forces and cease activities in both pore and ambient fluids (Hale et al., 1992). This was observed during the tests as the specimens in the solutions were swelled to various degrees before reaching equilibrium as illustrated by the change in their volume strains with time. Based on the double layer concept, the process of ionic exchange can be used to explain the expansion of the specimen in the $CaCl_2$ solution. As the ambient solution with the divalent cations Ca^{++} flows into the specimen, the cations from the solution enter the specimen in response to the concentration differences, and replace the interlayer cations. One Ca^{++} is capable of replacing two monovalent ions in the double layer. This may decrease the size of the double layer if the size of the Ca^{++} equal to that of the monovalent ions. Based on the ion exchange concept (Velde, 1992; Eick, 2000), the first preference for Ca^{++} is to replace Al^{+++}. This will allow the number of potassium cations that are weakly held in the pore fluid to increase their repulsive force and to give more space to calcium to settle in within the lattice structure of the specimen. In the meantime, the large diameter of Ca^{++} allows the clay crystals to move apart, causing an increase to the double layer and subsequent expansion to the specimen.

The same mechanism can also apply to the other ambient solutions. However, the only difference is that the presence of monovalent cations such as K^+ of the pore fluid and Na^+ from the ambient solution can increase the the concentration in the porespaces. This may force the balancing cations to move closer to the crystals and cause a reduction in the

repulsive force which in turns lead to a compression in the double layers. Both reduction and compression mechanism result in a decrease in the inter-layer particle space and greatly reduces the expansion of the specimen.

To explain the low swelling potential of the specimens in the *KCl* solution, two possible mechanisms are suggested. The first is the ion exchange reaction between cations of the specimens and that of the ambient fluid. The analysis of the clay minerals in Chapter 3 showed that mixed layer clay minerals are a repeated pattern of smectite and illite components. Due to the smaller negative lattice charge the smectites have, the K^+ in the ambient solution can easily be replaced by Na^+, Mg^{++}, and / or Al^{+++} in the lattice structure of the smectite hence the cations held in smectite are more loosely and some of them are exchangeable. The ongoing replacement results in more cations on the surface of the smectite and to a possible charge imbalance. The latter will lead to a reduction in the repulsive force within the specimen and between the specimen and the ambient fluid. The condition of apparent stabilization will enable the interlayer cations to stop H_2O from entering the specimen.

The second mechanism is a result of a development of a non-uniform repulsive force due to the ion exchange reaction between K^+ ions of the pore spaces and that of the ambient solution. In the absence of the confining stress, the non-uniform distribution force is capable of disturbing the cations on the crystal lattice, particularly at the surface of the specimen where repulsive force is the highest. This allows the solution to flow into the specimen and specimen swells. Specimen shows no more swelling when equilibrium between ambient solution and pore fluid is reached. The time for equilibrium is a prime factor in controlling the volume strain of the specimen.

The influence of effective stress change on these mechanisms cannot be predicted hence investigating the effects of different pore fluids on the Bringelly shale was under a steady ambient pressure. However, the relative contribution of suction and osmosis to the swelling cannot easily be determined from these tests as the *NaCl* concentration used was 58,000 *ppm*, which was much higher than the pore water concentration.

Based on the possible mechanisms discussed above, it is believed that the deposition environment of a lagoonal-coastal marsh sequence that characterize Bringelly shale (Herbert,1979), has played an important role in causing instability to the interlayer cations that are not tightly held in the lattice structure of the clay minerals. This may have caused the lattice structure of the deposits to accept cations that can be exchangeable as long as the net charge of the population balances the charge on the lattice structure of these deposits. However, cations such as Si, Fe, Al, and Mg are mostly permanent in the crystal lattice structure, and these are not readily substituted. This was evident from the response of the specimens tested in sodium and calcium chloride solution. Sodium and calcium have relatively larger size cations, so increase in the double layer is expected to be proportional to their sizes.

§4.6 **SUMMARY**

Laboratory measurements of commonly used index properties of Bringelly shale were carried out on block and core samples. The very low porosity of fresh Bringelly shale suggests that the material should perform satisfactorily as an engineering material. However, uncertainty about the nature and strength of the cementing agent of this material may cause the material to lack durability.

Saturated water content reflects the state of weathering whereby higher water contents are indicative of weathered shale. It was found that all samples of Bringelly shale were partially saturated. For Bringelly shale it was recommended that water content cannot be used as a direct measure of the porosity of shale and hence is a poor indicator of strength and stiffness. Water content indicates variation in saturation rather than variation in porosity.

Consistency tests for Bringelly shale indicated that the shale has the properties of a clay with low plasticity. The liquid limit of the crushed shale which increases from 30 for fresh shale to over 50 for extremely weathered shale is evidence for an increasing reactivity of the residual soil compared to the parent shale. This change in reactivity is

associated with changes in mineralogy. The durability of Bringelly shale seems to be influenced by the state of weathering encountered. The durability of Bringelly shale varies from medium for fresh intact rock to very low for highly weathered states.

Based on previous and current studies, fresh Bringelly shale can be categorized as strong rock. The study shows that for Bringelly shale there is a trend of decreasing strength with increasing water content, but there is great variation. The variation is a result of the partial saturation of Bringelly shale. Due to the low core recovery, difficulties were experienced in obtaining sufficient *UCS* data. Because of this limitation, it is believed that only the more cemented material is recovered and subsequently tested and the strength is possibly over-predicted.

Both diametral and axial point load tests have been performed on Bringelly shale. For Bringelly shale the anisotropy index has a mean of 3.0 while for Ashfield shale the mean is 2.0. The relatively high anisotropy index of Bringelly shale indicates that there is a much greater variation between axial and diametral point load strengths results for Bringelly shale, which is believed to reflect the varying extent of microcracking which is controlling its diametral strength.

To further investigate the mechanisms responsible for the slaking of Bringelly shale, tests were performed to assess the free and confined swell potential as well as the influence of pore fluid chemistry on the swelling of the shale. Much greater swelling strains are measured for Bringelly shale than Ashfield shale. This may partially be contributed to the presence of microcracks in Bringelly shale and their absence in Ashfield shale.

Swelling of Bringelly shale was also observed in a confined swell test as a result of reducing the effective stress at a consistent rate. Pore water suctions and osmotic effects due to differences in chemistry of pore fluid and swelling liquid can be used to describe mechanisms by which Bringelly shale is susceptible to swelling. Because of the presence of reactive mixed layer clays in the Bringelly shale, it has been expected that changes in pore fluid will contribute to volume changes. Tap water and calcium chloride cause the

most swelling and significant deterioration while the least swelling occurs with the potassium chloride solution, and no deterioration was observed when the shale was left in this solution for several days.

The swelling of Bringelly shale is size dependent. Swelling reduces as specimen size increases. The influence of pore fluid on swelling of Bringelly shale shows trends that are consistent with double layer interactions, and demonstrate the importance of pore fluid chemistry in controlling the magnitude of any swelling strains. It is suggested that swelling is a surface phenomenon related to disturbance. The extent of swelling in-situ needs further assessment. Nevertheless, the results indicate a significant swelling potential where construction activities result in water contacting the shale.

In order to investigate the reason for the high value of *UCS* of the natural Bringelly shale and the rapid disintegration of this material when placed in water, pore water suction was measured. The influence of saturation on the suction of Bringelly shale was investigated from the data on suction measured from the fully saturated Ashfield shale. The results showed the role of saturation in influencing the pore pressure suction of the natural shales.